IEEE Access
Multidisciplinary | Rapid Review | Open Access Journal

Date of publication xxxx 00, 0000, date of current version xxxx 00, 0000.

Digital Object Identifier 10.1109/ACCESS.2017.Doi Number

Classifications and Applications of Inkjet Printing Technology: A Review

Muhammad A. Shah[1,2], Duck-Gyu Lee[2], Bo-Yeon Lee[2] and Shin Hur[1,2] (Member, IEEE)

[1]Department of Nano-mechatronics, University of Science and Technology, Daejeon, 34113, South Korea.
[2]Korea Institute of Machinery and Materials, Daejeon 34103, South Korea.

Corresponding author: Shin Hur (e-mail: shur@kimm.re.kr).

This work was supported by the Technology Innovation Program (or Industrial Strategic Technology Development Program) (10078310, MO9500, Development of High-speed Multi-pass DTP System) funded by the Ministry of Trade, Industry & Energy (MOTIE, Korea), and the main research program (NK218D) funded by Korea Institute of Machinery and Materials (KIMM), and the Human Plus Convergence R&D Program (NB0070) funded by National Research Foundation of Korea.

ABSTRACT Inkjet printing technology uses the low-cost direct deposition manufacturing technique for printing and is applicable in various fields including optics, ceramics, three-dimensional printing in biomedicine, and conductive circuitry. This study reviews the classifications and applications of inkjet printing technologies, with a focus on recent publications. The different design approaches, applications, and research progress of several inkjet printing techniques are reviewed. Among them, the piezoelectric inkjet printing technology is the main focus owing to its reliability and handling of a diverse range of inks. A piezo-driven inkjet printhead is activated by applying a voltage waveform to a piezoelectric membrane. The waveform ensures the formation of the designed droplet and a stable jet. A survey of various driving-voltage waveforms is conducted, which can serve as a reference to the research community that uses piezo-driven inkjet printheads. The challenges of printing quality, stability, and speed and their solutions as published in recent studies are reviewed. Technologies for producing high-viscosity inkjets are explored, and the applications of inkjet printing technology in textile, displays, and wearable devices are discussed.

INDEX TERMS Inkjet Printing Technology, Printhead, Piezoelectric Inkjet Printing, Satellite droplet, Voltage Waveform

I. INTRODUCTION

Inkjet printing technology has applications in the fields of bioengineering [1], three-dimensional (3D) printing of microstructures [2], flexible and textile electronics [3], and micromechanical and microfluidic devices [4]. In 1858, William Thomson and Abbe Nollet invented an inkjet-like recording device with a continuous inkjet head [5], which paved the way for inkjet printheads. This technology was further matured by the introduction of the equations of fluid motion, drop-on-demand (DoD) inkjet heads with the squeeze, bend, push, and shear deformation modes using a piezoelectric actuator, and DoD thermal inkjet (TIJ) printheads [6].

Inkjet printing technology can be classified into two groups, continuous ink jet (CIJ) and DOD ink jet [6]. In a CIJ system, a stream of droplets is ejected continuously under an applied electric field and a charging electrode. The uncharged droplets are received by a catcher. In a DOD printing system, the droplet can be ejected by a voltage waveform. Referenced from [6] and further modified with information on the latest printing technologies. Fig. 1 shows the classification of inkjet printing technology.

Several methods including needle-based printing [7], piezoelectric [8] and thermal [9] inkjet printing, electrohydrodynamic (EHD) jet printing [10], laser-based printing [11], aerosol jet printing (AJP) [12], surface acoustic-waves (SAW) printing [13], acoustophoretic printing [14], and drop impact printing [15] were demonstrated.

All these methods have their merits and demerits that make it suitable for printing resolution, various materials and applications. For example piezoelectric, thermal, needle-based and acoustophoretic printing are nozzle-based methods that are prone to clogging when attempting to extend their use for printing the inks which can cause nozzle blockage. However, piezoelectric inkjet printing is the most mature and reliable technology [16]. The mechanical structure of a piezoelectric inkjet printhead (PIP) has an ink chamber connected to the ink cartridge through a narrow path called the restrictor or throttle. On top of the ink chamber is a

This article has been accepted for publication in a future issue of this journal, but has not been fully edited. Content may change prior to final publication. Citation information: DOI 10.1109/ACCESS.2021.3119219, IEEE Access

membrane composed of a piezoelectric material sandwiched between two electrodes. A nozzle supplies ink droplets to the outer substrate by applying an electrical pulse to the piezo-driven membrane on top of the ink chamber. This membrane pressurizes the chamber, increasing the fluid velocity at the nozzle. The high velocity of the fluid leads to droplet formation at the nozzle exit [16]. The piezoelectric membrane, ink chamber, and nozzle are manufactured on wafers using microelectromechanical systems (MEMS). These structures are combined using an MEMS-based bonding technique to fabricate a printhead device. The TIJ printhead consists of a resistor, a chamber and a nozzle. An electrical pulse applied to the resistor heats the fluid, forming a vapor bubble that pushes the fluid through the nozzle, thus producing a droplet or a series of droplets [16].

Several studies have reviewed inkjet printing technologies. Reference [17] reviewed various materials and the application of inkjet technology to print them. These technologies, ranging from PIP to EHD printing, have various applications in printing 2D or 3D materials at the micrometer and nanometer scales [18][19]. Reference [6] reviewed the history of PIP dynamics, covering the topics of actuation, ink chamber and nozzle acoustics, droplet formation, wetting, and air bubbles [6]. Li *et al.* [8] reviewed various piezo-driven inkjet printhead designs, along with their applications and challenges. Kwon *et al.* [20] reviewed commercially available printheads, ink supply systems, and inkjet printing technologies. Reference [21] explored microdroplet generation methods [21].

In this study, we focused on the classifications and applications of printing technologies. Focus is laid on the piezoelectric inkjet printing technology, especially the various voltage waveforms, the influence of voltage waveform on droplet formation, and methods to optimize these waveforms. Research articles that discussed the challenges related to the printing quality, stability, and speed of piezo-driven printheads and their solutions were articulated. Furthermore, high-viscosity jet ink printing technologies were discussed. Finally, various applications of different inkjet printing technologies in the fields of digital textile printing (DTP), display pixel printing, MEMS and wearable, stretchable, flexible devices were reviewed.

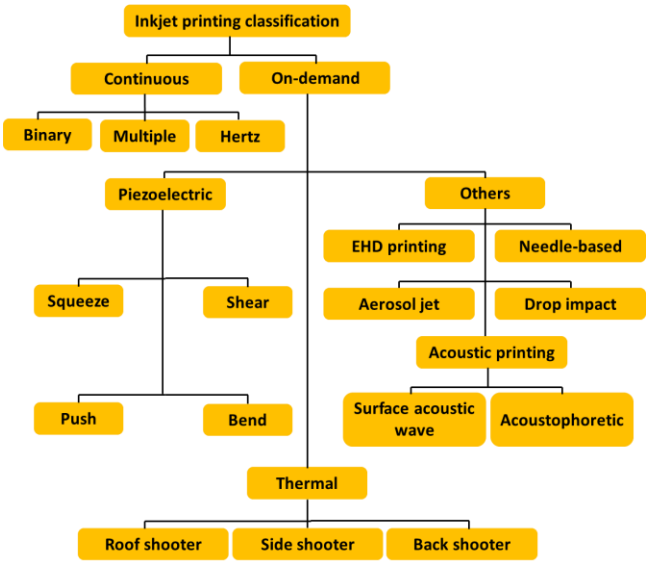

FIGURE 1. Classification of printing technologies [6].

II. TYPES OF INKJET PRINTING TECHNOLOGY

A. PIEZOELECTRIC INKJET PRINTING

In a PIP, the shape of the piezoelectric transducer changes under an applied voltage. This generates a pressure pulse in the ink chamber, resulting in the ejection of ink droplet from the nozzle connected with the chamber. A PIP can be in the squeeze, push, shear, or bend mode (Fig. 2). Most studies have demonstrated the bend mode.

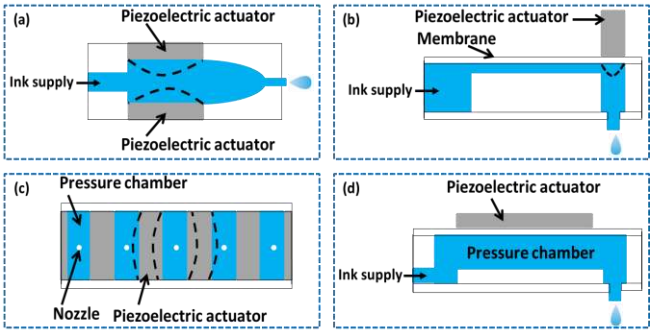

FIGURE 2. Classification of piezo-driven inkjet printheads. (a) squeeze mode, (b) push mode, (c) shear mode, (d) bend mode. The figure was referenced from reference [6].

1) ACTUATION MECHANISMS AND EFFECT OF VOLTAGE WAVEFORM

The PIP can be actuated by using either the push–pull (Fig. 3-a) or pull–push mode (Fig. 3-b). Generally, for these modes, a single trapezoidal pulse called the standard voltage waveform is used, which is composed of the rise, dwell, and fall times. At the rising edge of the pull–push mode, the piezoelectric membrane bends upward (z-axis), causing the ink chamber to expand and generate a negative pressure. Meanwhile, the ink is sucked from the nozzle and restrictor toward the center of the ink chamber. The membrane is still bent upward along the z-axis during the

This article has been accepted for publication in a future issue of this journal, but has not been fully edited. Content may change prior to final publication. Citation information: DOI 10.1109/ACCESS.2021.3119219, IEEE Access

dwell time. At the falling edge, the membrane bends toward the ink chamber, causing the chamber to contract and generate a positive pressure. Thus, the droplet is ejected from the nozzle exit. The push–pull mode works opposite of the pull–push mode, i.e., the membrane is pushed toward the ink chamber at the rising edge and bent upward in the z-direction at the falling edge of the voltage waveform. References [22][23] have studies the push–pull actuation mechanism [22][23], in which the jet pressure and ink droplet velocity are not affected by the change in the dwell time of the voltage waveform [23]. However, this mode has a low velocity. In the case of the pull–push mode, although the jet pressure and droplet velocity fluctuate with the dwell time, the velocity is high. Because printing applications require high jet velocities, researchers have focused on the pull–push actuation mechanism.

The ink chamber still undergoes pressure oscillations even after the first ink droplet has been ejected under an applied standard voltage waveform using the pull–push actuation mechanism [24]. These undesired pressure oscillations decay after several microseconds, cause variations in the properties of the subsequent ink drops, and form satellites, which degrades the inkjet printhead performance. A voltage waveform with two trapezoidal pulses to suppress the undesired pressure oscillations was formulated. Based on the polarity, the voltage waveform was divided into two categories by pulse type, unipolar [25][26] and bipolar [27][28]. In both the cases, the first pulse was used for jetting an ink drop, whereas the second one, with the same or opposite polarity, was used to damp the undesired pressure oscillations.

Kwon and Kim [25] used the waveform with unipolar pulses. They extracted the pressure wave information from the ink chamber using piezoelectric self-sensing measurement by measuring the piezo-current. The second pulse was used to suppress the undesired pressure oscillations. They set the magnitude of the second waveform to half that of the first one, which cancelled out the undesired pressure oscillations. The start time of the second waveform is highly sensitive to oscillations in the unipolar voltage waveform. The undesired pressure oscillations were suppressed with the optimal start time of the second pulse of 18.8 µs; however, if the start time were more or less than this threshold, then the jetting performance would be poor, or even worse than the single voltage waveform in the case of a decreased second pulse start time. In addition to the suppression of undesired pressure oscillations, the suppression of satellite droplet formation has also been demonstrated by using a voltage waveform with unipolar pulses [26]. The disadvantage of using this type of waveform is that it takes longer to dampen the undesired pressure oscillations than with the voltage waveform with bipolar pulses [29]. Therefore, mostly voltage waveforms with bipolar pulses have been used in the literature [27]–[30].

To obtain a better jet, the optimal parameters of the jet pulse must be determined. The optimal parameter can be defined as the highest possible velocity and sufficient volume of an ink droplet for a specific voltage waveform parameter at given amplitude. Generally, a voltage waveform with a rise and fall time of less than 3 µs is sufficient for good droplet ejection [31], however the dwell time must be considered. As the dwell time increases, the velocity and volume of the ink droplet increases. Above the optimal dwell time, it decreases drastically [32][33]. This trend also applies to the M-shaped, W-shaped, or other complex waveforms when tuning their time parameters. Different approaches were presented for estimating the optimal dwell time of a voltage waveform for achieving a higher droplet velocity and required volume. Reference [31] used the wave propagation theory and recommended an optimal dwell time of l/c [31], whereas [34] recommended $2l/c$, where l is the length of the tube and c is the speed of sound in inks. However, no accurate optimal dwell time exists in practice because l and c are likely to be unknown and the fluid viscosity effect cannot be considered without complicating the equation. Therefore, other methodologies, for e.g., numerical simulation [35], model based [23][29][36–38], automatic tuning [39], and experimental approaches [25][40] have also been recommended. Table II lists the studies that used these approaches along with their optimal waveforms parameters and optimization methods. Table I presents the different voltage waveforms and their effects on the printhead's performance.

The efficient deposition of different types of inks on a substrate is necessary in the inkjet industry for all applications. Therefore, it is necessary to have a mechanism to control droplet formation. The simplest method is to tune the voltage waveform. In the case of a fluid with low viscosity, the ejection of the first droplet from the nozzle outlet is followed by the formation of satellite droplets. High-velocity satellite droplets can combine to form a main droplet during flight to the desired spot on the substrate. However, low- velocity satellite droplets have poor directionality and may land on an arbitrary spot on the substrate, which reduces the print quality. Multipulse waveforms are needed to prevent satellite droplets and maintain the single primary droplet [41-46]. Shin *et al.* [41] applied a double waveform with two square pulses (unipolar M-shaped) to the actuator, which effectively ejected the single main droplet without forming satellites. The trajectory of the satellite droplets can be improved by tuning the separation time (t_4) between two pulses [42][43]. Reference [43] suppressed satellite droplets by tuning the time interval (t_2) of a unipolar W-shaped waveform [44].

Droplet with ligament is another challenge during printing, especially in applications that use a moving substrate. In this case, the ligaments will not merge with the main droplet. This will in turn misshape the printed dot on

This article has been accepted for publication in a future issue of this journal, but has not been fully edited. Content may change prior to final publication. Citation information: DOI 10.1109/ACCESS.2021.3119219, IEEE Access

the moving substrate [47]. Moreover, the length of the ligament increases as the applied voltage is increased. In the multidrop ejection method, a multipulse input voltage waveform is applied to the piezoelectric actuator. Applying different voltages to the pulses and tuning the pulse voltage can eliminate ligaments and satellites [47].

The quality of printing by inkjet technology has improved. Long-term productivity would require small droplets ejected at higher velocities. A dominant parameter, the droplet size can be reduced by reducing the nozzle orifice diameter and decreasing the pulse amplitude. However, a small orifice can be clogged and requires expensive manufacturing techniques. Moreover, decreasing the amplitude will decrease the droplet velocity. Therefore, alternative methods to reduce the droplet size must be researched. Reference [48] proposed three square-wave bipolar W-shaped voltage pulses with amplitudes of −46, 56, and −46 V, respectively. The method successfully reduced the droplet volume. The droplet volume can also be reduced by the M-shaped and bipolar waveforms; however, the W-shaped waveform has a higher percentage volume reduction effect than the two [42]. Fig. 3(c) illustrates the classification of the actuation mechanisms of a piezo-driven inkjet printhead and waveform optimization methods.

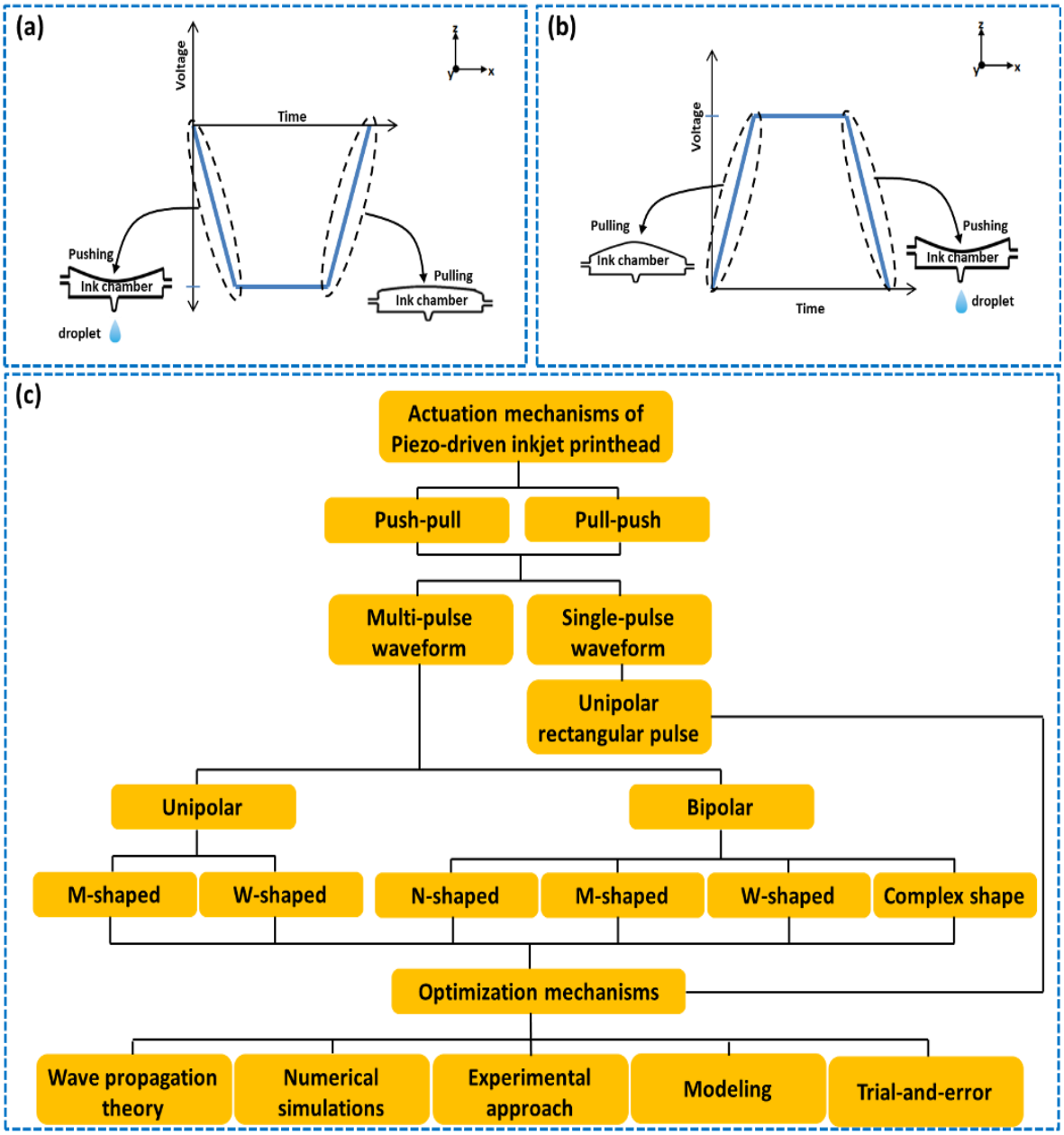

FIGURE 3. Schematic representation of (a) push–pull, (b) pull–push modes, and (c) classification of actuation mechanisms of a piezoelectric inkjet printhead with the waveform optimization approaches.

TABLE I
VARIOUS VOLTAGE WAVEFORMS AND THEIR EFFECTS ON PRINTHEAD PERFORMANCE

Voltage waveforms		Comments
Single pulse	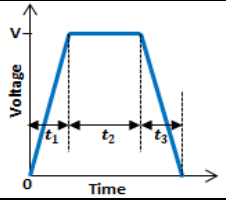	• For efficient droplet ejection, t_1 and t_3 must be less than 3 μs [31]. • Optimal value of t_2 can be obtained through experiment, theory, simulation, or modeling.
Unipolar M-shaped	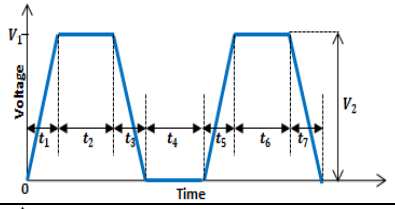	• In this waveform, the 1st pulse plays the same role as the unipolar single pulse waveform. • The 2nd pulse can be used to suppress residual oscillations [14] and satellite droplets [43]. • This waveform can be used to reduce the droplet volume [39]. • The time interval t_4 must be optimal as it is sensitive to both residual oscillations and satellite droplets.
Bipolar M-shaped	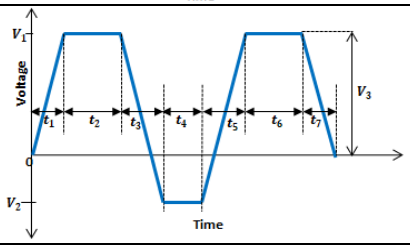	
Unipolar W-shaped	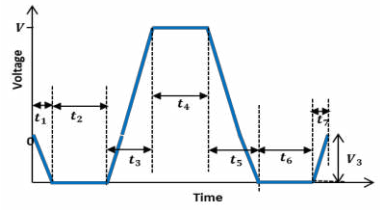	• This waveform can be used to reduce the droplet volume [48]. • In a unipolar W-shaped waveform, the satellites can be suppressed by tuning time interval t_2 [44].
Bipolar W-shaped	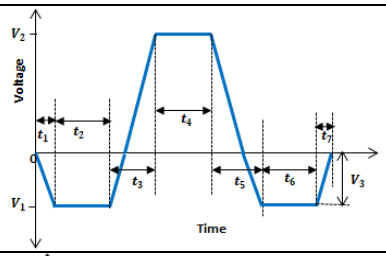	
Bipolar-1 N-shaped	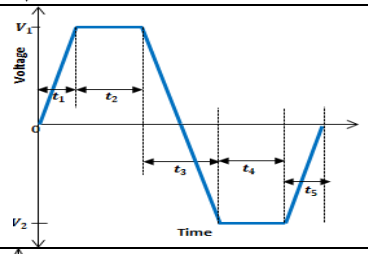	• The 2nd pulse of this waveform is used to suppress the residual vibrations. • This waveform can be used to eject highly viscous inks as it allows for a high voltage difference [43]. • The droplet velocity and volume decrease and subsequently increase as t_4 increases [49].
Bipolar-2 N-shaped	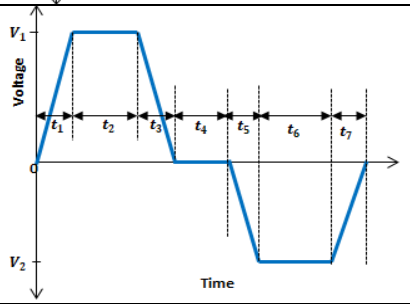	• The 2nd pulse of this waveform is used to suppress residual vibrations. • Time interval t_4 is designed to allow the chamber pressure to reach its minimum.

TABLE II
OPTIMIZED VOLTAGE WAVEFORMS AND THEIR OPTIMIZATION METHODS

Waveform	Authors and References	Ink's Viscosity (cP)	Optimal Parameters (μs)	Drop Volume (pL)	Drop Velocity (m/s)	Method
Unipolar single pulse	Bogy & Talke [31]	16.1	t_2: 8.2	Not Available	3.5	Wave propagation theory
	Wei *et al.* [35]	10	t_2: 15–18	Not Available	6	Numerical simulations
Unipolar M-shaped	Won & Kim [25]	9	t_2: 3 t_4: 9.8	Not Available	Not Available	Experimental approach
Bipolar-1 N-shaped	K.S. Won [27]	NA	t_2: 20 t_4: 40	Not Available	Not Available	
Bipolar-2 N-shaped	Khalate *et al.* [29][50]	10	t_1: 2 t_2: 2.5 t_3: 1.3 t_4: 7.6 t_5: 1.3 t_6: 0.4 t_7: 4.4	Not Available	5–9.8	Model based
	Wang *et al.* [30]	1.19	t_1, t_3, t_5, t_7: 3 t_2, t_6: 24 t_4: 17	Not Available	Not Available	
Bipolar M-shaped	Snyder *et al.* [39]	0.45	t_1: 2 t_2: 3 t_3: 7 t_4: 0 t_5: 6 t_6: 1 t_7: 10	1.1	1.83	Automatic tuning

2) MISCELLANEOUS STUDIES AND RECENT RESEARCH IN PIEZOELECTRIC INKJET PRINTHEADS

Although piezoelectric inkjet printheads are commercial, the printing quality and jet stability can be improved ~~to solve~~ by solving the nozzle clogging, the nonaxisymmetric effect, and the entrainment of air bubbles in the ink channel.

The clogging of a nozzle strongly influences the inkjet printhead performance in various applications. For example, sieving, bridging, and aggregation of particles can block the flow of fluid in microfluidic devices [51]. The unconventional MEMS printhead process causes dirt particles composed of Si or glass to remain in the ink channel. The interaction of these remaining dirt particles with the oscillating meniscus, or cavitation in the bulk ink, cause the entrainment of air bubbles in the tube [52]. For example, the collision of silica with the internal surfaces of a printhead can clog the nozzle [53]. Nozzle blockage can be minimized by tuning the pH of silica sol [53]. Reference [53] visualized the growth, translation, and interaction of the entrained air bubbles using shortwave infrared imaging [54]. Nozzle blockage can also be solved by ink recirculation. A recirculation system can enhance the reliability of the jet and remove the entrapped air bubbles [20].

Another issue with piezoelectric inkjet printheads is the nonaxisymmetric effects, which degrade the stability and performance of inkjet printhead. A nonaxisymmetric droplet can prevent the capturing of satellite droplets as they diverge from the trajectory of the main droplet. High-frequency jets can reduce the nonaxisymmetry effects as it forces the successive droplet to follow the first jetted asymmetrical droplet. The causes and their solutions must be researched to improve the printhead's performance and stability. Nonaxisymmetry can be caused by the misalignment of the printhead channel with the nozzle plate, dust particles at the nozzle surface, wetted nozzle plate, bubble trapped inside the nozzle, and unstable asymmetrical surface modes at the meniscus interface by a Rayleigh–Taylor-like mechanism [55]. Fig. 4 illustrates various axisymmetric droplets [55]. Furthermore, jet stability can be improved by cooling the ink [56].

Satellite droplets degrade the print quality and reproducibility. These droplets are formed by the breakage of the long ligament behind the main droplet. As mentioned earlier, a method to suppress satellite droplets is to tune the voltage waveform. Another method is to add viscoelasticity to the ink. Sen *et al.* [57] suppressed satellite droplets in water-based ink by infusing polymers. The addition of polymers stabilizes the ligament against the Rayleigh–Plateau instability. The ligament was pushed toward the main droplet, producing a single droplet without satellites [57]. Reference [56] suppressed satellite droplets by cooling the ink [56].

Wettability of the nozzle's inner wall and surface tension of the ink are the two main factors affecting the quality and speed of the droplet. The breakup time can be delayed and the droplet velocity can be reduced by increasing the contact angle of the ink with the nozzle inner wall. Meanwhile, the droplet can be broken up earlier and accelerated by increasing the surface tension [58]. The printing quality can be improved by selecting high-surface-tension inks and modifying the nozzle inner wall to make it hydrophilic.

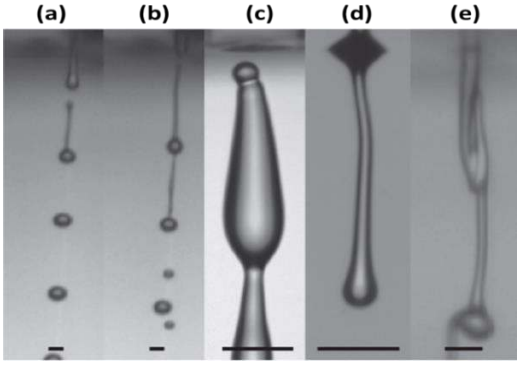

FIGURE 4. Different axisymmetric droplets [55]. (a) divergent droplet trajectory, (b) setallites jetting away from the main droplet, (c) tail droplet pushed toward the nozzle edge, (d) deflection of the droplet toward the nozzle wall, and (e) asymmetry effect of the first axisymmetrical droplet on the second droplet during high frequency jetting.

B. THERMAL INKJET PRINTING

The TIJ can be in the form of a roof-shooter, side-shooter, or suspended heater [59]. In the first configuration, the heater is placed behind the nozzle. In the second configuration, it is placed adjacent to the nozzle. In the third configuration, the heater is suspended within the ink chamber [59]. Most industries manufacture and utilize the roof-shooter TIJ [60]. Fig. 5 illustrates the three forms of TIJ.

The major problem with the TIJ printhead is its short lifetime because of the electromigration of the heater, damage by bubble cavitation, and thermal stress-induced cracks [9][61]. The lifetime can be increased by increasing the thickness and shape of the heater [9][61][62]. Another problem is *kogation* [63], a phenomenon where ink particles are deposited on the heater surface during the operation of the TIJ, affecting the formation of bubble and droplet ejection. The addition of anions to ink can prevent this phenomenon [64].

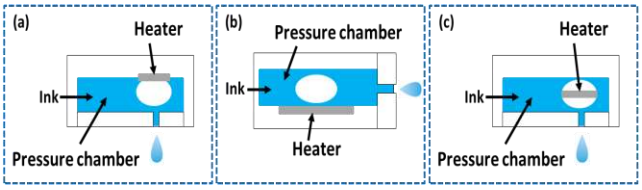

FIGURE 5. Three types of thermal inkjet printheads, (a) roof-shooter, (b) side-shooter, (c) suspended heater. The figure was referenced from [60].

C. ELECTROHYDRODYNAMIC JET PRINTING

In EHD jet printing, ink is ejected from the nozzle exit by a high applied electrical field between the nozzle and the substrate. Depending on the electric field, the EHD printing can be performed in the CIJ mode or DOD mode. The CIJ mode requires a constant DC supply between the nozzle and the substrate, whereas the DOD mode requires pulsed DC voltage. The DOD mode has been a focus area because its jet emissions can be controlled. Three different methodologies, AC [65], pulsed DC [66], and single potential AC [67], shown in Fig. 6, were demonstrated by studies related the DOD mode under an applied electric field. In the case of AC or pulsed DC, the electric potential is applied to the nozzle and the substrate is grounded, whereas the AC voltage is applied to the substrate and the nozzle is kept electrically floating in the case of single potential AC.

Various materials have been successfully printed on different substrates using EHD [68-73]. However, issues such as liquid wetting, particle–substrate interaction, and low throughput persist [74][75]. These challenges can be solved by changing the electrode shape, hydrophobic coating of the nozzle, and tuning the applied voltage and fluid flow rate [74]. Wu *et al.* [76] demonstrated an EHD printing system driven by a triboelectric nanogenerator (TENG). They claimed that the TENG can protect the substrate against the conventional high-voltage supply system. An array of nozzles can be used to solve the problem of low throughput [77]–[79]; however, the electrostatic crosstalk between the neighboring nozzles degrades the printhead's performance [80]–[82]. Several studies were conducted to suppress crosstalk. For example, researchers attempted to increase the space between nozzles. However, this can cause jet offset, especially in electrospinning [83]–[85]. Zhang *et al.* [86] confirmed that the linear arrangement of nozzles produced better uniformity in the jetted materials than the toothed nozzle arrangement.

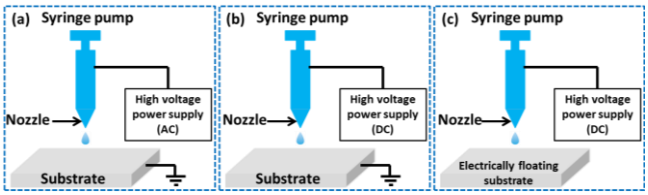

FIGURE 6. Electrohydrodynamic (EHD) jet printing systems with (a) AC, (b) pulsed DC, and (c) single potential AC. The figure was referenced from [67].

D. NEEDLE-BASED PRINTING

The key components of the needle-based printing system are needle, seat, and nozzle (Fig. 7). Air pressure [87] or a piezoelectric-stack actuator [88] can be used to move the needle. The actuator exhibits rapid response and high efficiency [89]. However, the piezo-stack actuator does not produce adequate output displacement for fluid jetting;

therefore, a displacement amplification mechanism, i.e., a mechanical amplifier (e.g., a lever) was adopted for the needle and actuator [90]. The two types of actuators are single [91] and dual [92] piezo-stack actuators. The dual piezo-stack actuator is used for high-viscosity and high-frequency jetting. The quick response of the actuator accelerates the needle movement [88][93]. Droplets are ejected from the nozzle exit by the motion of the needle toward the inside of the seat. The output parameters associated with the motion of the needle can be predicted through fluid flow simulations [94][95] or modeling [96]–[100]. Phung and Kwon [87] used the accelerometer to sense the needle motion. They also investigated the effects of various parameters on the motion and jetting behavior.

Various displacement amplification mechanisms were demonstrated to enhance the printing performance. For example, for the stress relaxation of a dual piezo-stack actuator, [101] presented the jetting dispenser based on a corner-filleted hinge attached to the actuator. The design was further improved in terms of the stress reduction in the actuator by introducing a cylindrical pivot and changing the shape of the amplifier block [102]. Zhou *et al.* [103] demonstrated a rhombic mechanical amplifier that exhibited a higher needle stroke than traditional mechanical amplifiers. Furthermore, the jetting performance can be enhanced by changing the needle shape. For example, the jetting velocity was increased by adding a side cap [104] and pin joint [105] to the needle.

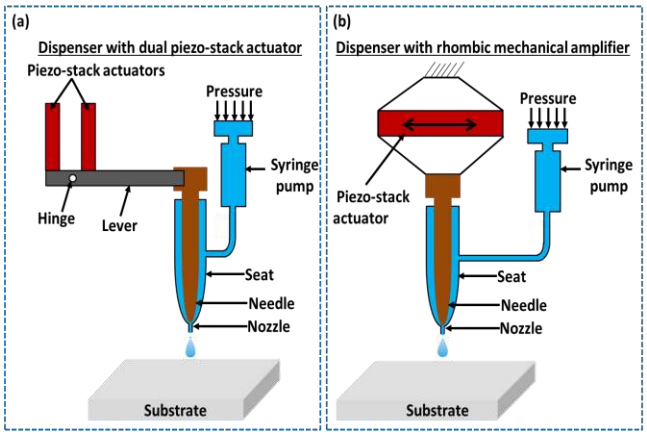

FIGURE 7. Needle-based dispenser system with (a) dual piezo-stack actuator and (b) rhombic mechanical amplifier. The figure was referenced from [103].

E. AEROSOL JET PRINTING

AJP is a high-resolution direct-writing droplet-based technique that can print a variety of materials with viscosities ranging approximately from 1–2500 cP [106]. This method was successfully applied in the fabrication of interconnects [107], sensors [108]–[110], organic light emitting diodes [111], supercapacitors [111], transistors [112], and medical imaging devices [113]. AJP works on the principle of the atomization of ink by ultrasonification or pneumatic mechanism, which results in aerosol formation (suspension of liquid particles in a gas carrier). The aerosol is then transferred to the deposition head by an inert gas stream (e.g., N_2), after which it is ejected from the nozzle exit. Sheath gas is added to the deposition head to further improve the performance. In an ultrasonic atomizer, the atomization of ink occurs from the generation of high-frequency pressure waves by the piezoelectric ultrasonic transducer. In the case of a pneumatic atomizer, an atomizer nozzle is placed in an ink reservoir where a carrier gas with a high velocity is passed through the tip of the atomizer nozzle, atomizing the ink. Fig. 8 illustrates an aerosol jet with both the atomization methods. Both methods have their merits and demerits. Compared with the pneumatic atomizer, the ultrasonic atomizer produces uniform aerosol; however, it can only print very high-viscous inks [114].

To achieve optimal aerosol-jet printing with improved performance, the relevant parameters must be tuned including sheath gas flow rate (SHGFR) and carrier gas flow rate (CGFR), which are the two main parameters of AJP that influence the quality of the printed line. The printed line width decreases by increasing the focusing ratio (SHGFR/CGFR) [115]. The ideal operating window for deriving the optimal parameters has not yet been defined owing to the complex structure of AJP and a lack of research in this area. Trial-and-error strategies have been adopted to achieve enhanced printing quality [115][116]. However, this approach is time consuming and inefficient. Modeling approaches that are faster, more efficient than trial-and-error methods, e.g., computational fluid dynamics model [106] and knowledge transfer framework [117], were proposed to predict these parameters for printing performance enhancement.

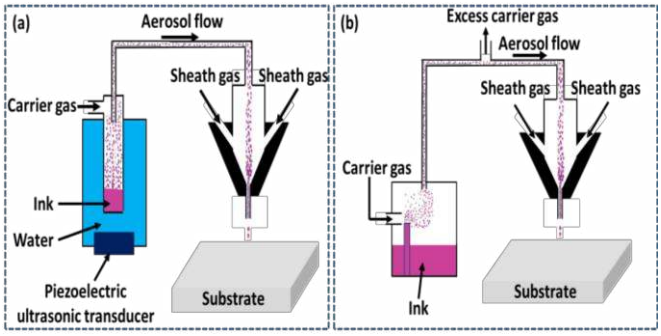

FIGURE 8. Aerosol jet printing system with (a) ultrasonic atomizer and (b) pneumatic atomizer. The figure was referenced from [12].

F. LASER-ASSISTED PRINTING

Laser-assisted printing system is composed of a laser beam and a special type of substrate called the donor substrate, the top of which is coated with an absorbing layer and the bottom side with an adhesive layer of ink, as shown in Fig. 9 [118]. The laser beam energy cavitates the ink layer, propelling the droplet to the collecting substrate [119]. Laser-assisted printing is a nozzle-less technique, and therefore, does not suffer from clogging. This technology is

used for direct writing [120] and DOD printing [121]. Various materials, e.g., conductive inks [122], adhesives [123], and biomaterials [124], were printed using this technology.

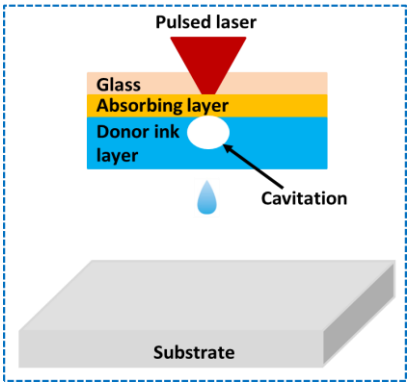

FIGURE 9. Laser-assisted printing system. The figure was referenced from [118].

G. ACOUSTIC PRINTING

The application of acoustic waves to propel an ink droplet is referred to as acoustic printing. The pioneering work of Elrod *et al*. [125][126] has led major research work in the field of acoustic printing. Scientists are developing various acoustic droplet-ejection methods [127][128]. Acoustic printing is further categorized into surface acoustic wave (SAW) and acoustophoretic printing.

1) SURFACE ACOUSTIC WAVE PRINTING

In SAW printing, the acoustic waves are generated at the surface of the liquid to propel the droplet. Generally, in a SAW-driven jet, interdigital transducers (IDTs) are patterned on a piezoelectric substrate. The substrate contracts and expands by applying radio frequency (RF) power to the IDTs, generating pressure waves of higher frequencies. The droplet is ejected by the acoustic radiation force generated from the SAW [129]. The IDTs can be connected on either side, which will drive the liquid along the Rayleigh angle (θ_R), or on opposite sides, which causes the droplet to be ejected on a point perpendicular to the printing surface, if the opposite sides have the same energy [130][131]. Furthermore, a pair of aligned IDTs can enhance the maximum jet speed and minimum jet time [132]. A schematic of the SAW-propelled jet with a pair of IDT electrodes is illustrated in Fig. 10.

Because the SAW-driven printing technique is nozzle-less, it does not have the clogging-related demerits of nozzle-based printing techniques. This is especially advantageous for printing with bio-inks. However, most SAW-driven printing devices do not allow flexible the tuning of the droplet size using the same device. To solve this problem, [133] demonstrated a pulsed SAW device to control the droplet size by changing the pulse width. The droplet size and velocity can also be controlled by changing the input RF power. Strong capillary waves at the droplet surface overcome the capillary stress and result in the atomization of the droplet as the RF power is further increased [134].

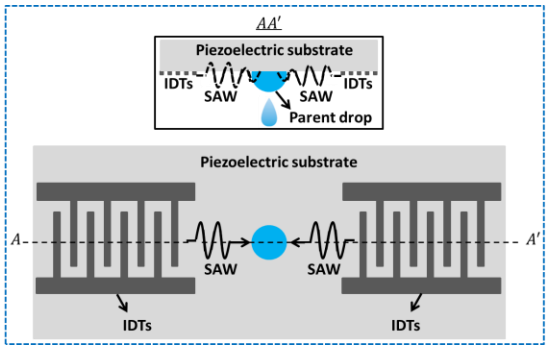

FIGURE 10. Schematic representation of surface acoustic wave printing system. The figure was referenced from [129].

2) ACOUSTOPHORETIC WAVE PRINTING

Reference [14] devised an acoustic nozzle-based printing mechanism, especially to print with highly viscous liquids. The mechanism uses three devices, actuator, acoustic cavity, and nozzle. The actuator was connected at one end of the acoustic cavity and activated by a driving ultrasonic frequency of approximately 25 kHz. The ink was injected at a constant flow rate into the nozzle inlet . The nozzle outlet was adjusted inside a Fabry–Pérot (FP) resonator in the location with the maximum acoustic pressure, as depicted in Fig. 11-a. The acoustophoretic force is generated in the FP resonator to detach the droplet flowing through a nozzle. Jetting occurs when the acoustic (F_a) and gravitational forces (F_g) exceed the capillary force (F_c), as shown in Fig. 11-b. For high acoustophoretic fields, the accuracy of the droplet trajectory decreases as the acoustic force increases. The droplet size can be decreased by increasing the acoustic force. The acoustic force can be calculated by integrating the radiation pressure p_{rad} over the surface S of the sample, as follows [14],

$$F_a = \int_S p_{rad} \vec{n} dS \tag{1}$$

where $\vec{n}$ is the normal component inward to S. The radiation pressure p_{rad} has a direct relation with the root-mean-square acoustic pressure and acoustic particle velocity, which can be increased by applying a voltage to the actuator. In other words, the droplet volume can be decreased by increasing the voltage applied to the actuator.

Various materials with a wide range of Z number (the inverse of the Ohnesorge number), including water, honey, bio-inks, and liquid metals have been printed successfully. Honey (viscosity: 25 000 cP) was printed on white chocolate. A low viscosity (2 cP) metal ink composed of eutectic gallium–indium (eGaIn) was also printed. These printed materials are depicted in Fig. 11-c and 11-d, respectively.

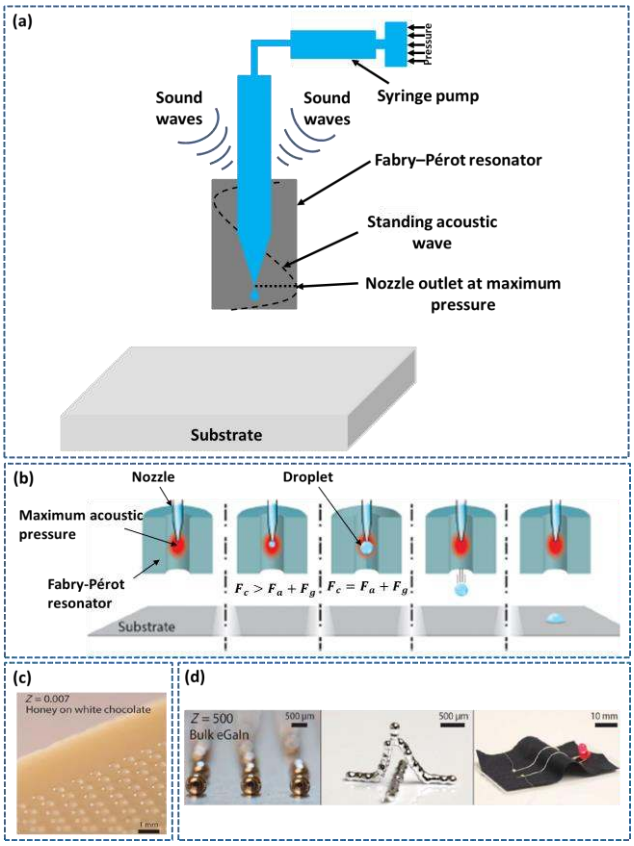

FIGURE 11. **Schematic representation of (a) acoustophoretic printing system, (b) acoustophoretic printing droplet detachment system, which demonstrates droplet detachment when the acoustophoretic and gravitational forces exceed the capillary force. (c) and (d) show the printed droplets of honey on white chocolate and a metal ink composed of eutectic gallium-indium (eGaIn), respectively. The figure was referenced from [14].**

H. DROP IMPACT PRINTING

Reference [15] proposed a DOD printing technique in which they replaced the nozzle with a sieve and dispensed a single satellite-free micrometer-sized droplet. The size of the jetted droplet was proportional to the pore size. The droplet size can be decreased by decreasing the pore opening. This technique can print for Z values ranging from 3–200. The size can be further improved in the case of printing highly viscous inks ($Z < 3$). Materials for biological and electronic applications were printed using this technique. The printing mechanism is illustrated in Fig. 12.

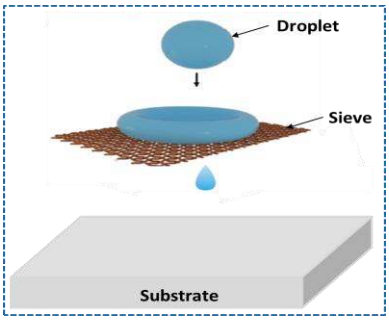

FIGURE 12. **Schematic ofthe mechanism of a drop impact printing system. The figure was referenced from [15].**

III. PRINTING TECHNOLOGIES FOR HIGH-VISCOSITY INKS

Viscosity governs the droplet formation in the inkjet printing process. The substrate's surface condition has a weak effect on the printed patterns of high-viscosity inks. A large force is required to eject droplets of these inks from the nozzle exit. In a piezo-driven inkjet printhead, high-viscosity inks can be ejected by actuating the piezo-membrane using a double bipolar voltage waveform instead of a single voltage waveform [43]. Jackson *et al.* [135] demonstrated a technique that used the XAAR 1003 recirculating inkjet printhead with a shear-mode actuator to eject high-viscosity inks. Due to the high fluid-recirculation rate, the printhead could eject ink with a viscosity of up to 98 cP.

The piezo-driven inkjet printheads cannot jet the ink with high viscosity; therefore, other approaches must be used, e.g., EHD [136], which was used for direct writing techniques or droplet jetting [137]-[139]. In this technique, the ink inside the printhead must be charged for better electrostatic deflection, which requires it to be conductive. However, high-viscosity inks have a lower conductivity, which leads to poor electrostatic deflection [140]. Laser-based printing can also be used to jet high-viscosity inks [11][122][123][141]. Zhang *et al.* [141] performed direct writing of alginate solutions of a viscosity 8279 cP. Therodorakos *et al.* [122] performed droplet-based jetting of Ag nanoparticles with an effective viscosity of 590 cP in a diethylene glycol monobutyl ether solvent. Needle-based dispensers are another device to produce high-viscosity ink jets. The motion of the needle toward the nozzle in the ink chamber causes the droplets to form a jet at the nozzle exit.

The literature contains various studies related to needle-based dispensers for the jetting of high-viscosity inks [142]–[145]. The jetting of high-viscosity ink can be improved by increasing the radius of the needle. Lu *et al.* [144] achieved the jetting of a 58 000-cP adhesive with a droplet volume of 0.6 µl, a needle radius of 1.5 mm, and a nozzle orifice diameter of 0.1 mm. Aerosol jet printing is a highly preferred method of direct writing. AJP can print inks with a viscosity of 1–2500 cP [146]. Recently, Forestri *et al.* [14] presented an acoustophoretic printing method for forming jets of droplets with very-high-viscosity inks at the nozzle exit. The acoustophoretic printer consisted of a Fabry–Pérot resonator and an acoustic source. Most acoustic waves were reflected because of the mismatch in the acoustic impedance at the fluid–air interface. Standing waves are generated in the resonator. A spherical droplet is ejected from the nozzle exit by the acoustophoretic force. Various inks with viscosities ranging from 0.5–25 000 cP were successfully printed using this approach.

Table III summarizes the methods to high-viscosity ink jets by the technology (piezoelectric, EHD, needle-based, laser, aerosol jet, and acoustophoretic printing). The table also lists the high-viscosity jetted materials and their

printing mechanisms. Among the methods, the acoustophoretic printing mechanism was found to be the simplest, most accurate for forming very-high-viscosity ink droplet jets. The use of MEMS to manufacture acoustophoretic printers will enable printing with high-frequency ink jets.

TABLE III
Summary of High-viscosity Inks Printing

Printing technology	Materials	Viscosity (cP)	References	Approaches
Piezo-Driven	Ultracur3D ST 30 LV	98	[135]	Droplet Based
EHD	Copper Paste	4000	[139]	Direct Writing
	Silver Paste	4000	[136]	
Laser-Assisted	Alginate Solutions	8279	[141]	Direct Writing
	Cyanoacrylate Adhesives	1700	[123]	Droplet Based
	Silver Nanoparticles	590	[122]	
	Hydrogel	431	[11]	
Needle Type	Glue	58 000	[144]	Droplet Based
	Glycerol	1412	[145]	
Aerosol Jet	Not Available	2500	[146]	Direct Writing
	Silver Nanoparticles	160	[12]	
Acoustophoretic	Honey	25 000	[14]	Droplet Based

IV. APPLICATIONS OF INKJET PRINTING

The conventional semiconductor fabrication process consists of several steps (from oxidation to photoresist removal) for manufacturing a single device, whereas the inkjet printing technique offers maskless lithography and involves fewer steps [147]. The conventional process and inkjet printing method are illustrated in Fig. 13. Various industries have been researching the application and translation of inkjet printing in manufacturing owing to its low cost, fewer steps involved, and low material loss. Studies have explored its application in printed electronics [148], chemical sensors [149], supercapacitors [150], carbon nanotubes [151], pharmaceuticals [152][153], and conductive materials [154]. The focus of this section is the application of inkjet printing technology in DTP, display pixel printing, MEMS, and wearable, flexible, and stretchable devices. Table IV summarizes the recent literature on the applications of various printing techniques.

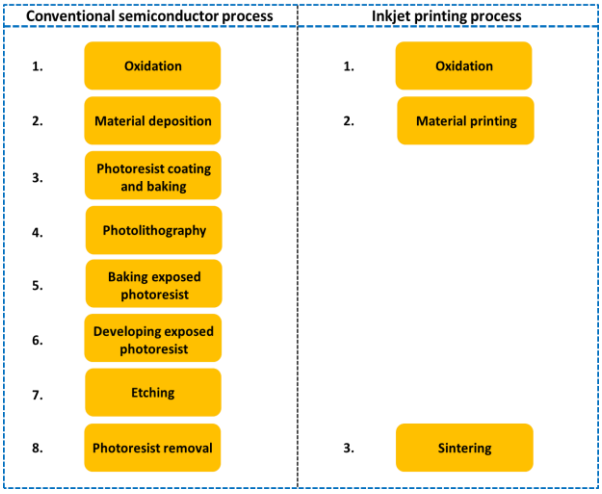

FIGURE 13 Fabrication steps of conventional semiconductor device fabrication and inkjet printing method. The figure was adopted from [147].

A. DIGITAL TEXTILE PRINTING

Inkjet printing technology, also referred to as digital printing, is widely used in various applications, including textile and graphic arts, that relied on conventional printing devices including rollers and screen printers until recently. Textile printing has grown rapidly with inkjet printing technology. This technology produces less waste, and consumes 45% less electricity and 35% less water compared with conventional printing technologies [155].

As inkjet printing is a non-contact process, the jetted droplets spread on contacting the substrate surface. The spreading of droplets on the substrate will affect the quality of the printed product [156]. The impact of droplets on various substrate surfaces with phenomena such as spreading, splashing, receding, and bouncing has been demonstrated [157]–[162]. The interaction of droplets on textiles in DTP has drawn significant research interest. The spreading and coalescing of droplets can affect the image quality printed on fabrics [163]. Zhang *et al.* [164] demonstrated the impact of aqueous glycerol droplets on hydrophobic and hydrophilic nylon textiles. The results demonstrated that the droplet penetrated and formed liquid filaments beneath the textile surface. They also concluded that the spherical shape of the droplet on the textile does not change when it interacts with porous substrates with a pore size from 100–300 μm in short time periods. Reference [165] analyzed the penetration of droplets in polyester fabric pores with and without an underlying substrate. The spreading ratio of water–glycerol droplets on the substrate is different with and without the underlying substrate because of the volume loss of the liquid [165].

Environment, pretreatment, and posttreatment affect the color and its performance. The process must be conducted in a controlled environment to improve the efficiencies of the printer. For example, reactive dyes require a humid

environment to develop a stronger bond with the fabric [166]. Acid and reactive dyes require streaming as posttreatment for bonding with fibers [166]. Pretreatment is often required to improve the DTP's performance. Various pretreatment agents and methods were demonstrated [167]–[170]. Reference [167] used commercially available pretreatment agents (DP-300 & DP-302 from Lubrizol Corporation) and demonstrated improved color intensity and gamut for pigment-based ink by pretreating cotton and polyethylene terephthalate fabrics. They used chemical padding as a pretreatment method. Kim *et al.* [168] used acrylic polymers as a pretreatment agent to improve the color of nylon fabrics. Li *et al.* [169] improved the color quality of a cotton/polyamide fabric substrate by pretreating it with alpha olefin sulfonate and sodium alginate. An *et al.* [171] improved the color performance by a combined process that used the protease enzyme and sodium alginate for wool fabric inkjet printing using reactive dyes.

Various studies have researched and developed materials for inkjet printing for printing on fabrics. Song *et al.* [172] synthesized RR218@PSBV by the absorption of RR218 (red dye 218) onto PSBV (poly (styrene-butyl acrylate-vinylbenzyl trimethylammonium chloride) nanospheres and inkjet-printed it on cotton fabric, as shown in Fig. 14-a. The dye@copolymer nanosphere improved the color performance, image quality, and material conservation [172]. In [173], two reactive red dyes, RR218 and reactive red 24:1 were inkjet-printed and the resulting droplets were compared. RR218 had more stable droplets and a smaller spread area (high resolution) than reactive red 24:1 [173]. Gao *et al.* [174] inkjet-printed dye-based inks on polyester fabric and investigated the effect of viscosity, surface tension, and fluidity on the sharpness of the printing pattern. Fig. 13-b displays a sample polyester fabric printed with dye-based inks. Various other studies were conducted to improve the performance of DTP by printing dye or pigment-based inks on different fabrics [175]–[179].

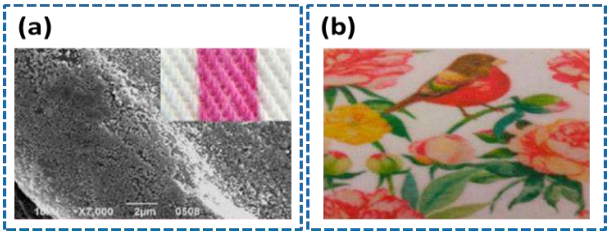

FIGURE 14. (a) Dye@copolymer (RR218@PSBV) printed on cotton fabrics [172]. (b) inkjet-printed dye ink on polyster fabric [174].

B. DISPLAY PIXEL PRINTING

Display technology has a ubiquitous effect in daily life. There are various types of displays [180]. For example, organic light emitting diode (OLED) has become a mainstream display technology as it consumes less power, is flexible, has a high contrast ratio, and is ultra-thin [181]. OLED is made of an emissive layer (EML) sandwiched between two conductors. A hole transport layer (HTL), hole injection layer (HIL), electron transport (ETL), and electron injection layer (EIL) can be added to enhance its efficiency [182]. Fig. 15-a displays the cross-sectional view of all the layers along with the electrodes**.** A cross-sectional schematic of red, green, and blue (RGB) pixel inkjet printing is illustrated in Fig. 15-b. The applications of OLED include computer, laptop, automobile, TV, and mobile phone displays. Several methods including spin coating, transfer printing, lithography, evaporation, and inkjet printing are used to deposit multilayer thin films of OLED.

Inkjet printing offers a significant advantage in the field of display electronics because it offers maskless lithography, consumes less material, uses a simple fabrication technique, and has larger substrate scalability. Therefore, it has been adopted for the fabrication of OLED displays. We focus on the latest studies on OLED fabrication using inkjet printing. In [183], a 3-in blue OLED array was inkjet-printed, resulting in improved uniformity of the surface [183]. Yoon *et al.* [184] used an ink with various solvents to print the emissive layer of the OLED. Thus, they achieved a uniform film. Zhaobing *et al.* [185] inkjet-printed an EML, HTL, and HIL for an OLED and achieved uniformity. However, the device efficiency requires further improvement. An image of the inkjet-printed green EML layer is displayed in Fig. 15-c. Reference [186] inkjet-printed a poly(3,4-ethylenedioxythiophene):poly(styrenesulfonate) (PEDOT:PSS) HIL, with polyethylene glycol (PEG) for improved efficiency and bending resistance of the OLED device.

Another study printed a PEDOT:PSS (dissolved with isopropanol and ethylene glycol) HIL using a multi-nozzle inkjet printing system [187]. They achieved uniform droplet ejection by changing the solvent and tuning the printing parameters. Amruth *et al.* [188] printed an EIL made of a cesium carbonate film (with an alcohol-based solvent) for a polymer OLED. The current efficiency and luminance were enhanced compared to an OLED without the film. Researchers printed micro-lenses for pixelated OLEDs to enhance the out-coupling efficiency [189][190]. Reference [192] printed 31-in [191] and 55-in [192] active matrix OLED (AMOLED) displays, improving the performance of the display technology.

Quantum dot light-emitting diode (QLED) is another display that can be printed by inkjet technology. These LEDs have long lifetime, low power consumption, high contrast, wide color gamut, wide viewing angles, and high refresh rate [193][194]. Kim *et al.* [195] inkjet-printed an octane-based QD ink for a green OLED. They tested various mixtures of solvent with the octane-based QD ink and found that the octane–cyclohexane mixture was the most stable. Chen *et al.* [196] printed highly efficient red QLEDs using a QD ink based on a mixture of n-tridecane

and decalin solvents. Quantum dots can also be used as color-conversion layers in display technologies. Lin *et al.* [197] effectively suppressed the blue residual light by inkjet-printing QD inks. Hu *et al.* [198] fabricated a 6.6-in QLED display with a QD layer printed to eliminate the blue residual emissions. They demonstrated a reduction in the transmittance of the residual blue light by increasing the thickness of the QD pixel layer. Yang *et al.* proposed the application of a Bragg reflector with an inkjet-printed QD pixel layer to further increase the color conversion efficiency. The reflector was composed of a multilayer of silicon oxide / titanium oxide.

Perovskite quantum dots (PQDs) have become a significant area in display technology research owing to their distinct optical properties, including a tunable wavelength and narrow emission wavelength [199]. Shi *et al.* [200] inkjet-printed PQD inks with water as a solvent. Yoo *et al.* [201] printed with a perovskite ink on an ethyl cellulose film and concluded that a (3-aminopropyl) trimethoxysilane (APTES)-coated red perovskite ink had improved drying stability. Other studies reported improvement in color [202] and brightness [203] by inkjet-printing with PQD inks with various solvents.

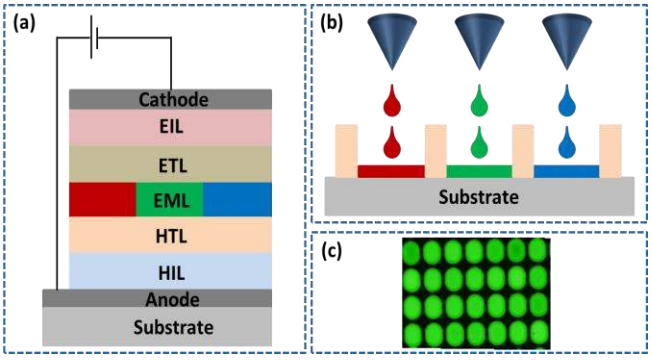

FIGURE 15. Display technology with (a) cross-sectional view of the layers of OLED display, (b) schematic cross-sectional view of inkjet red, green, blue (RGB) pixel printing, and (c) inkjet-printed green emissive layer (EML) [185].

C. MEMS DEVICES PRINTING

Inkjet printing is also considered a versatile technique in the manufacturing of MEMS devices because it is environmentally friendly, produces less waste, is maskless, and offers rapid and multimaterials deposition [204].

1) PHOTOLITHOGRAPHY

In photolithography, a photoresist material can be applied using various coating techniques. These coating techniques still has flaws, among which photoresist material wastage is one [205]. Inkjet printing can be used to deposit the photoresist materials to overcome this problem [206]. Bietsch *et al.* [207] deposited alkanethiolate monolayers and DNA oligonucleotides on Au films using inkjet printing. Fukushima *et al.* [208] inkjet-printed acrylic resin on Al. Qu *et al.* [209] used the EHD technique to print photoresist lines; the line width was controlled by the voltage supplied to the substrate and nozzle. Bernasconi *et al.* [210] inkjet-printed SU-8-2005, an epoxy-based photoresist material. This material cannot be printed in it pristine form by commercially available piezoelectric inkjet printheads owing to its higher viscosity. To decrease the viscosity, the material was diluted with cyclopentanone (CP), tetrahydrofuran (THF), and N-methyl-1-pyrrolidone (NMP). The jetting of SU-8-CP and SU-8-NMP was found to be stable, whereas that of SU-8-THF was not because of the partial blockage of the nozzle [210]. The authors claimed that the partial blockage was due to the lower boiling point of THF, i.e., it evaporates, leaving partially solidified SU-8 at the nozzle's meniscus. This can cause a misdirected jet.

Micro-lenses and micro-lens arrays play a vital role in various applications, including optical communications, optical storage devices, wavefront sensing, and biomedical instruments. Inkjet printing is widely used in micro-lens and micro-lens array fabrication. Compared with photolithography, inkjet printing can deposit various materials at precise locations on any substrate for the fabrication of micro-lenses [212]–[218].

2) ETCHING

Inkjet printing can be used to remove the small areas with predeposited films. The advantage of inkjet etching is minimal material wastage. The dielectrics of SiO and Si_3N_4 were inkjet-etched by ejecting an NH_4F solution onto a polyacrylic acid film, which produces HF [219]. Another interesting application of inkjet printing is polymer etching. Microstructures with varying shapes (concave to convex) can be prepared on top of polymer surfaces [220][221]. Microstructures with microgrooves, microwells, and hexagonal holes were also fabricated using inkjet etching. The dimensions of these microstructures can be controlled by tuning the jetted droplet volume, modifying the polymer–solvent interaction, substrate temperature, and processing parameters [222].

In addition, inkjet printing has been used to fabricate thin-film transistors (TFTs) [223]. For example, Kim *et al.* [224] fabricated a TFT by inkjet-etching Ag. Etchant (a mixture of ferric nitride and deionized water) was impinged on the surface of Ag by etching Ag films with a thickness of 20–80 nm, which generated a source–drain electrode. Li *et al.* [225] fabricated a TFT array wholly by inkjet printing pure Cytop solvent on a Cytop layer.

3) DEPOSITION

Direct material deposition is the most common application of inkjet printing in the fabrication of MEMS devices. A variety of different materials, including conductive, insulator, sacrificial, piezoelectric, and two-dimensional (2D) materials, can be deposited [226]. Piezoelectric materials play a vital role in the manufacturing of MEMS sensors, actuators, energy storage devices, transformers, and transducers. Various studies were published on the direct deposition of piezoelectric materials by inkjet

printing. Kuscer *et al.* [227] deposited lead zirconate titanate (PZT) thick films onto a platinized alumina substrate by inkjet printing. Ink was formed by dispersing PZT particles in a water–glycerol mixture. However, they observed a few defects in the deposited film [227]. Subsequently, they synthesized defect-free structures by adding polybenzoxazole (PbO) to the aqueous ink [228]. Godard *et al.* [229][230] deposited a thin-film PZT onto a platinized silicon substrate. Pabst *et al.* [231] demonstrated all-inkjet-printed of micropump actuator. Zheng *et al.* [232][233] fabricated 3D microstructures of ice by impinging water droplets onto an existing ice structure, after which the droplets immediately froze.

The application of signal path to the MEMS devices is performed by electrical conductors. The various inkjet-printed conductive inks, their electrical characterization and applications, and historical background were reviewed by [154]. Godard *et al.* [234] printed Ag as the top electrode on a thin-film PZT layer. In [231], both the top and bottom electrodes of Ag in a piezoelectric micropump actuator were deposited by inkjet printing.

Reference [235] fabricated entire MEMS electrostatic drive motor was fabricated by inkjet printing (Fig. 16). They used Au and Ag nanoparticle inks to fabricate the motor structure. The insulator (polyketone resin) was inkjet-printed to electrically isolate the Au and Ag electrode wires. Delekta *et al.* [236] presented a fully inkjet-printed graphene-based microsupercapacitor, in which the electrodes were made of graphene, and the electrolyte nanographene oxide. Kaneto *et al.* [237] demonstrated an MEMS capacitive sensor for humidity. The sensor was fabricated by combining transfer and inkjet printing. Graphene oxide (GO) nanoparticles were deposited by printing them on Au electrodes, which was prefabricated on a PET substrate by screen printing. This bilayered GO/Au thin film exhibited higher Young's modulus than the Au thin film.

4) MEMS PACKAGING

Optical and electrical interconnects and adhesives for sealing and bonding in MEMS packaging can be printed by inkjet printing [238]. In the 3D packaging of MEMS devices, through-silicon via (TSV) is mostly used as an interconnect structure for signal transmission. Studies were published regarding the conductive plating and filling of vias by inkjet printing. Khorramdel and Mantysalo [239][240] demonstrated the inkjet-printing of an Ag-nanoparticle ink for the partial filling of a TSV. Quack *et al.* [241] developed ink-jetted Au-filled TSV arrays. Yang *et al.* [242] deposited Ag and filled a via at a lower processing temperature and electrical resistivity, and further enhanced its electrical performance [243].

Khorramdel *et al.* [244] stated that the partial metallization of a TSV by inkjet printing was not sufficiently mature for volume production. Therefore, they used an alternate approach that involved filling a hollow metallized TSV with a dielectric polymer and depositing an Ag ink as an under-bump metallization (UBM) pad, as shown in Fig. 17. Both the dielectric polymer and metallic ink were inkjet-printed. Solder balls of SnAgCu-based inks were also impinged on top of the UBM pads. Two commercialized printheads, i.e., piezoelectric and EHD, were used for printing metals and polymers [244]. Roshanghias *et al.* [245] inkjet-printed redistribution layers (RDLs) and a metal route used to connect the MEMS microphone pads to application-specific integrated circuits (ASICs) and fan-out the signals via solder balls. In another study, they inkjet-printed the RDLs of Ag-ink nanoparticles for the fan-out packaging of capacitive micromachined ultrasound transducers [246]. Other studies have demonstrated the synthesis of adhesives by inkjet printing [247][248].

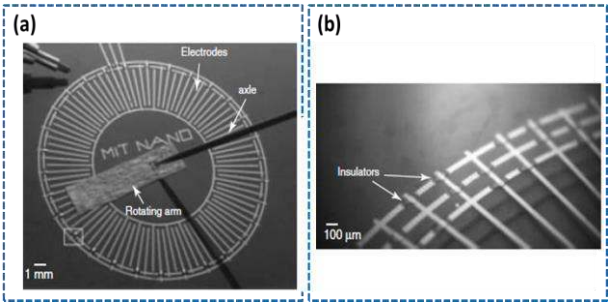

FIGURE 16. **(a) All-inkjet-printed MEMS electrostatic drive motor. (b) inkjet-printed layer of resin to electrically isolate Au and Ag electrodes [235].**

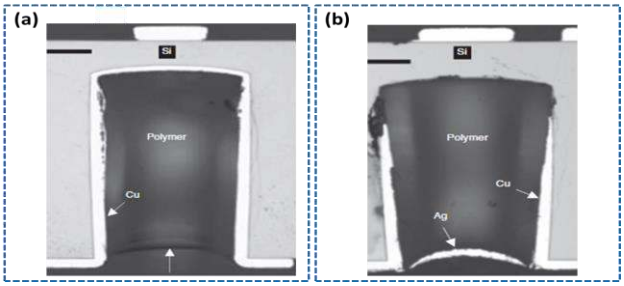

FIGURE 17. **Cross-sectional images of inkjet-printed (a) dielectric polymer, and (b) UBM layer of silver ink [244].**

D. WEARABLE, FLEXIBLE, AND STRETCHABLE DEVICES

Wearable, flexible, and stretchable (WFS) devices have achieved remarkable progress in smart devices and healthcare modality [249][250]. These devices can be directly mounted on the human skin or attached to fabrics. Novel device fabrication approaches are required to achieve, and retain, high performance. Inkjet printing has various applications in fabricating WFS devices and circuits due to its low cost, material wastage, fewer steps, maskless working, and precise deposition of small droplets on the substrate surface [251][252]. Inks consisting of dielectric, conductors, and semiconductors can be printed on fabrics

and skin by inkjet printing. For example, Ag nanowires and nanoparticles were printed for flexible and stretchable electronics [253]–[257]. Mikkonen *et al.* [258] demonstrated an all-inkjet-printed electrical circuit device (Fig. 18). Both the conductive (Ag nanoparticles) and dielectric (polydimethylsiloxane (PDMS)) materials were jetted by inkjet printing. PDMS was used as a dielectric between the conductive tracks [258]. Wang *et al.* [259] developed an all-inkjet-printed flexible proximity sensor (Fig. 19-a). Both ZnO and web-shaped top electrodes (Ag nanoparticles) were jetted on a flexible Al sheet used as a bottom electrode. Another all-inkjet-printed wearable device for electronic textiles (e-textiles) applications was proposed in [260]. They printed a graphene–Ag composite ink on a piece of cotton fabric.

The human body temperature provides information about health status. Wearable temperature sensors are used to measure this temperature. Inkjet printing can be used to devise wearable temperature sensors. Kuzubasoglu *et al.* [261] jetted an aqueous carbon nanotube (CNT) conductive ink to fabricate a wearable temperature sensor. Vuorinen *et al.* [262] demonstrated a temperature sensor by printing graphene/Poly (3,4-ethylenedioxythiophene):poly (styrenesulfonate) (PEDOT:PSS) ink on a skin-conformable polyurethane substrate. Fig. 19-b displays the photograph of the sensor printed on a subject's finger. Reference [264] used CNT/PEDOT:PSS composite ink to fabricate a temperature sensor [263]. Wang *et al.* [264] presented an all-inkjet-printed PEDOT-PSS-based temperature sensor with PEDOT:PSS as the sensing layer, fluorinated polymer (CYTOP) as the passivation layer, and Ag nanoparticles as the electrode. High stability in humidity was achieved for the sensor by introducing CYTOP as the passivation layer (Fig. 19-c).

In addition, inkjet printing was used to fabricate respiratory rate stretchable and wearable sensor [265][266], piezoelectric devices [267][268], piezoresistive devices [269][270], and bio-impedance sensors for electrical impedance tomography imaging [271]. Electronic circuits for WFS devices were also printed by inkjet printing [272]–[275].

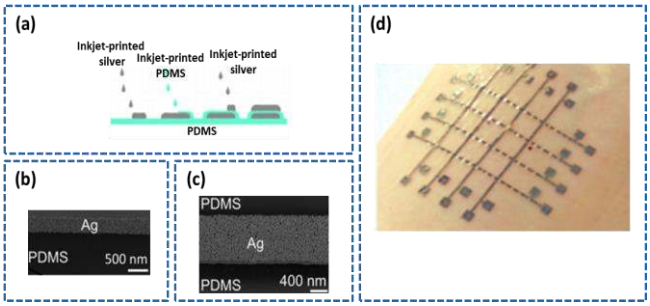

FIGURE 18. **All-inkjet-printed multilayer electrical device (a) cross-sectional view, (b) topmost inkjet-printed silver layer of the intersection, (c) bottommost inkjet-printed silver layer of the intersection, and (d) all-inkjet-printed device. The figure was referenced from [258].**

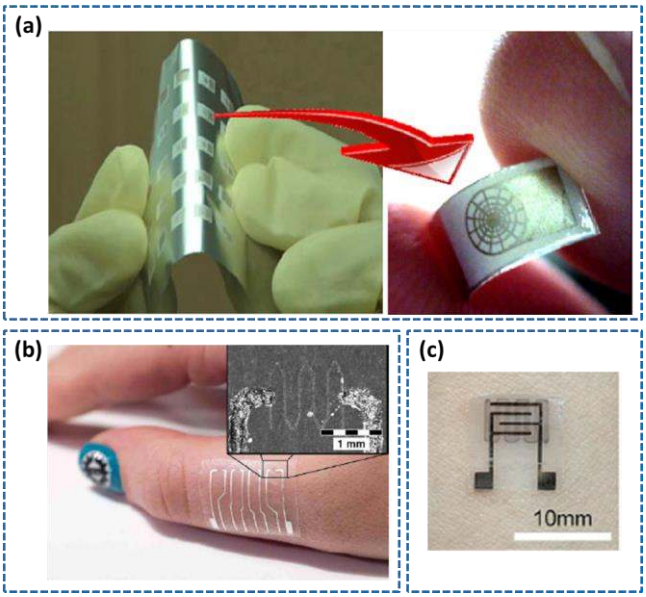

FIGURE 19. **Inkjet-printed (a) proximity sensor [259], (b) temperature sensor array [262], and (c) temperature sensor attached to the human skin [264].**

TABLE IV
SUMMARY OF RECENTLY PUBLISHED STUDIES ON APPLICATIONS OF INKJET PRINTING TECHNIQUES

Printing mechanism	Reference	Year	Materials	Applications
Piezoelectric inkjet	[172]	2020	Reactive red 218 dyes + Poly (styrene-butyl acrylate-yinylbenzyl trimethylammonium chloride)	Textile printing
Piezoelectric inkjet	[174]	2021	Dye based ink	Textile printing
Piezoelectric inkjet	[186]	2020	Poly(3,4-ethylenedioxythiophene):poly(styrenesulfonate) (PEDOT:PSS) + Polyethylene glycol	OLED display technology
Piezoelectric inkjet	[187]	2021	PEDOT:PSS + Isopropanol +	OLED display technology

			Ethylene glycol	
Piezoelectric inkjet	[235]	2002	Gold (Au) and silver (Ag) nanoparticles, polyketone resin (insulator)	MEMS electrostatic drive motor
Piezoelectric inkjet	[224]	2019	Mixture of ferric nitride and deionized water	Thin-film transistors
Piezoelectric inkjet	[231]	2014	Poly(vinylidene fluoride-co-trifluoroethylene) (P(VDF–TrFE)), Ag electrodes	Piezoelectric actuator as a pump in microfluidic lab-on-chip systems
Piezoelectric inkjet, EHD jet	[244]	2017	Ag, dielectric polymer, SnAgCu-based inks	Through-silicon via as an interconnect in MEMS packaging
Piezoelectric inkjet	[236]	2019	Graphene, nanographene oxide	Microsupercapacitor
Piezoelectric inkjet	[259]	2010	Zinc oxide, Ag-nanoparticles	Flexible proximity sensor
Piezoelectric inkjet	[258]	2020	Ag-nanoparticles, Polydimethylsiloxane (PDMS)	Silicone rubber-based multilayered electronics
Piezoelectric inkjet	[260]	2019	Graphene-Ag composite ink	Wearable electronic textile
Piezoelectric inkjet	[263]	2021	Carbon nanotube/PEDOT:PSS	Wearable human body temperature sensor
Piezoelectric inkjet	[276]	2020	Graphene	Tactile sensor
Piezoelectric inkjet	[264]	2020	PEDOT-PSS, Fluorinated polymer, Ag-nanoparticles	Wearable human body temperature sensor
Piezoelectric inkjet	[277]	2021	Ag-nanoparticles	Flexible dielectric-barrier-discharge plasma actuator
Piezoelectric inkjet	[278]	2021	Poly(vinylidene fluoride-trifluoroethylene) (P(VDF-TrFE))	Ultrasonic applications
Piezoelectric inkjet	[279]	2021	Nanoporous carbon	Microsupercapacitor devices
Piezoelectric inkjet	[280]	2021	Poly(3-hexylthiophene) (P3HT), poly(vinylpyrrolidinone) (PVP), PEDOT:PSS	Pressure sensor
Piezoelectric inkjet	[281]	2021	8 mol% Y2O3-stabilized ZrO2 (8YSZ) ceramic ink	Thin film layer of electrolyte in solid oxide fuel cell
Piezoelectric inkjet	[282]	2021	Benzocyclobutene-base polymer ink	Electronic applications
Piezoelectric inkjet	[283]	2021	Aluminum–oxide dielectric precursor ink ($Al(NO_3)39H_2O$, Merck, 99.997%)	Resistive switching devices
Piezoelectric inkjet	[269]	2021	Ag nanoparticles	Flexible sensor for deflection monitoring
Piezoelectric inkjet	[284]	2021	Ag nanoparticles	Flexible heaters
Piezo-stack based droplet generator	[215]	2015	Ultraviolet polymer	Micro-lens arrays
Thermal inkjet	[285]	2021	Silica aerogel	Thermal insulating layers in microelectronic chips and batteries
Thermal inkjet	[286]	2021	Ag nanowires	Printed electronics
Thermal inkjet	[287]	2021	Solutions of geobacillus stearothermophilus (*G. stearothermophilus*) & bacillus atrophaeus (*B. atrophaeus*) spores	Time temperature indicator for drug and food industry
Thermal inkjet	[288]	2021	MXene	Wearable textile electronics
Aerosol jet	[109]	2021	Graphene	Ammonia gas sensor
Aerosol jet	[110]	2021	Ag, polyaniline	Ammonia gas sensor
Aerosol jet	[113]	2021	Hybrid halide perovskite $CH_3NH_3Pbi_3$	X-ray photodetector in medical imaging applications
Aerosol jet	[289]	2021	Ag, kapton, NaCl	Microfluidic flexible force sensors
Aerosol jet	[111]	2021	Ag-nanowire, PEDOT:PSS	OLED display technology
EHD jet	[290]	2021	Molybdenum disulfide (MoS_2)	Thin film transistors
EHD jet	[291]	2021	Graphene, polymer	Photodetectors
EHD jet	[292]	2021	Ag-nanoink	Biomedical imaging
EHD jet	[293]	2021	Silicone ink	Dielectric elastomer actuator in tunable lenses
EHD jet	[268]	2021	Polyvinylidene fluoride (PVDF), single-walled carbon nanotubes (SWCNTs)	Flexible piezoelectric pressure sensor for human motion detection
EHD jet	[209]	2019	BP212 photoresist	Photoresist structures fabrication
EHD jet	[275]	2021	Ag-nanoparticles	Wearable electronics circuits
EHD jet	[294]	2021	Pluronic F127 (PF-127), gelatin methacryloyl (GelMA) hydrogel	Microvascular tissue for biomedical applications

VI. CONCLUSION

Inkjet printing technology is used in various industries from textiles and display technology to biomedicine owing to its simple process, shorter process time, and low material consumption with digital control and non-contact printing method. It is necessary to develop and mature different

printing methods for printing variety of inks to manufacture multifunctional devices. We discussed the types of inkjet printing technologies and their applications, namely PIP, TIJ, EHD, needle-based printing, AJP, laser-assisted printing, acoustic printing, and drop impact printing. Due to the nozzle-less nature of laser-assisted, acoustic and drop impact printing technologies, they do not have the clogging-related demerits. The advantage of needle-based, AJP and EHD printing methods is that it can print high viscosity inks. Despite the piezoelectric inkjet printing technology, all other techniques are still on developing stage and many features of these technologies need to be matured to make it suitable for commercial applications. Among the discussed printing technologies, the piezoelectric thin-film-driven inkjet printing technique is matured and employs a diverse range of inks. Lower printing cost, easy optimization of the printing conditions and faster printing speed of the piezoelectrinc printing method makes it advantageous compared to other printing technologies. By easy optimization, we mean the droplet size and speed can be optimized easily by only tuning the driving voltage waveform. Recently, this technology has been used in flexible electronic devices, DTP, and display technology because it allows for the controlling of droplet jetting, volume, and velocity through voltage waveforms. The conventional inkjet printhead cannot form ink jets greater than 10 cP. Although studies have attempted to heat the ink and reduce its viscosity by producing jets from the printhead, this approach is not compatible with very high-viscosity inks. Therefore, this review analyzed the inkjet printing techniques for dispensing high-viscosity inks. EHD, aerosol jet, and acoustophoretic printing are used to print high-viscosity inks in direct writing and DOD. The applications of inkjet printing in digital textile, display pixel, MEMS device, and wearable, flexible, and stretchable device printing were discussed, and the application principle and method were analyzed. The recent, most promising application fields are DTP, which is environmentally friendly and can be directly printed on fabric, OLED and quantum dot display technologies, and flexible electronics. This review emphasizes the effective inkjet printing technologies for researchers studying the field or working in relevant applications.

In the case of piezoelectric inkjet printheads, designs with ink-recircualtion are needed to improve their performance. Developing new printing technologies, especially for printing high viscosity inks, are the need in future perspective. MEMS technology can further leads the printing devices to reduced footprint. The acoustophoretic printing device can further be improved in terms of high frequency jetting if it is manufactured using MEMS technology.

REFERENCES

[1] P. Kumar, S. Ebbens, and X. Zhao, “Inkjet printing of mammalian cells – Theory and applications,” *Bioprinting*, p. e00157, Jun. 2021.

[2] S.-Y. Wu, C. Yang, W. Hsu, and L. Lin, “3D-printed microelectronics for integrated circuitry and passive wireless sensors,” *Microsystems Nanoeng.*, vol. 1, p. 15013, July. 2015.

[3] T. Carey *et al.*, “Fully inkjet-printed two-dimensional material field-effect heterojunctions for wearable and textile electronics,” *Nat. Commun.*, vol. 8, no. 1, Oct. 2017.

[4] P. Cooley, D. Wallace, and B. Antohe, “Applications of ink-jet printing technology to BioMEMS and microfluidic systems,” *JALA - Journal of the Association for Laboratory Automation*, vol. 7, no. 5. pp. 33–39, Oct. 2002.

[5] H. Wijshoff, “Structure and fluid-dynamics in piezo inkjet printheads,” Ph.D. dissertation, Oce Technologies B.V. R&D, Univ. of Twente, Enschede, Netherlands, 2008.

[6] H. Wijshoff, “The dynamics of the piezo inkjet printhead operation,” *Physics Reports*, vol. 491, no. 4–5. pp. 77–177, Jun. 2010.

[7] T. H. Phung and K. S. Kwon, “How to manipulate droplet jetting from needle type jet dispensers,” *Sci. Rep.*, vol. 9, no. 1, Dec. 2019.

[8] H. Li, J. Liu, K. Li, and Y. Liu, “Piezoelectric micro-jet devices: A review,” *Sensors Actuators, A Phys.*, vol. 297, p. 111552, Oct. 2019.

[9] J. H. Lim *et al.*, “Failure mechanisms in thermal inkjet printhead analyzed by experiments and numerical simulation,” *Microelectron. Reliab.*, vol. 45, no. 3–4, pp. 473–478, Apr. 2005.

[10] D. Gao and J. G. Zhou, “Designs and applications of electrohydrodynamic 3D printing,” *International Journal of Bioprinting*, vol. 5, no. 1. 2019.

[11] M. Gruene, C. Unger, L. Koch, A. Deiwick, and B. Chichkov, “Dispensing pico to nanolitre of a natural hydrogel by laser-assisted bioprinting,” *Biomed. Eng. Online*, vol. 10, Mar. 2011.

[12] R. R. Salary, J. P. Lombardi, D. L. Weerawarne, P. K. Rao, and M. D. Poliks, “A state-of-the-art review on aerosol jet printing (AJP) additive manufacturing process,” in *ASME 2019 14th International Manufacturing Science and Engineering Conference, MSEC 2019*, Erie, PA, USA, 2019, vol. 1.

[13] C. Fu *et al.*, “Vertical jetting induced by shear horizontal leaky surface acoustic wave on 36° Y-X LiTaO3,” *Appl. Phys. Lett.*, vol. 110, no. 17, Apr. 2017.

[14] D. Foresti *et al.*, “Acoustophoretic printing,” *Sci. Adv.*, vol. 4, no. 8, Aug. 2018.

[15] C. D. Modak, A. Kumar, A. Tripathy, and P. Sen, “Drop impact printing,” *Nat. Commun.*, vol. 11, no. 1, Aug. 2020.

[16] J. F. Dijksman, "Introduction," in *Design of Piezo Inkjet Print Heads : From Acoustics to Applications*, 1st ed., Wiley, 2019.

[17] P. Calvert, “Inkjet printing for materials and devices,” *Chemistry of Materials*, vol. 13, no. 10. pp. 3299–3305, Sept. 2001.

[18] C. Ru, J. Luo, S. Xie, and Y. Sun, “A review of non-contact

micro- and nano-printing technologies," *Journal of Micromechanics and Microengineering*, vol. 24, no. 5. Apr. 2014.

[19] M. S. Onses, E. Sutanto, P. M. Ferreira, A. G. Alleyne, and J. A. Rogers, "Mechanisms, Capabilities, and Applications of High-Resolution Electrohydrodynamic Jet Printing," *Small*, vol. 11, no. 34. pp. 4237–4266, Jun. 2015.

[20] K. S. Kwon, M. K. Rahman, T. H. Phung, S. D. Hoath, S. Jeong, and J. S. Kim, "Review of digital printing technologies for electronic materials," *Flexible and Printed Electronics*, vol. 5, no. 4. IOP Publishing Ltd, p. 043003, Dec. 2020.

[21] Y. Y. WEI, Z. Q. SUN, H. H. REN, and L. LI, "Advances in Microdroplet Generation Methods," *Chinese Journal of Analytical Chemistry*, vol. 47, no. 6. Chinese Academy of Sciences, pp. 795–804, Jun. 2019.

[22] B. H. Kim, H. S. Lee, S. W. Kim, P. Kang, and Y. S. Park, "Hydrodynamic responses of a piezoelectric driven MEMS inkjet print-head," *Sensors Actuators, A Phys.*, vol. 210, pp. 131–140, Apr. 2014.

[23] M. A. Shah, D. G. Lee, and S. Hur, "Design and characteristic analysis of a MEMS piezo-driven recirculating inkjet printhead using lumped element modeling," *Micromachines*, vol. 10, no. 11, p. 757, Nov. 2019.

[24] M. A. Shah, D. G. Lee, B. Y. Lee, N. W. Kim, H. An, and S. Hur, "Actuating voltage waveform optimization of piezoelectric inkjet printhead for suppression of residual vibrations," *Micromachines*, vol. 11, no. 10, p. 900, Sep. 2020.

[25] K. S. Kwon and W. Kim, "A waveform design method for high-speed inkjet printing based on self-sensing measurement," *Sensors Actuators, A Phys.*, vol. 140, no. 1, pp. 75–83, Oct. 2007.

[26] B. H. Kim, S. Il Kim, J. C. Lee, S. J. Shin, and S. J. Kim, "Dynamic characteristics of a piezoelectric driven inkjet printhead fabricated using MEMS technology," *Sensors Actuators, A Phys.*, vol. 173, no. 1, pp. 244–253, Jan. 2012.

[27] K. S. Kwon, "Waveform design methods for piezo inkjet dispensers based on measured meniscus motion," *J. Microelectromechanical Syst.*, vol. 18, no. 5, pp. 1118–1125, Oct. 2009.

[28] J. Chung, S. Ko, C. P. Grigoropoulos, N. R. Bieri, C. Dockendorf, and D. Poulikakos, "Damage-free low temperature pulsed laser printing of gold nanoinks on polymers," *J. Heat Transfer*, vol. 127, no. 7, pp. 724–732, Jan. 2005.

[29] A. A. Khalate, X. Bombois, R. Babuška, H. Wijshoff, and R. Waarsing, "Performance improvement of a drop-on-demand inkjet printhead using an optimization-based feedforward control method," *Control Eng. Pract.*, vol. 19, no. 8, pp. 771–781, Aug. 2011.

[30] J. Wang, J. Huang, and J. Peng, "Hydrodynamic response model of a piezoelectric inkjet print-head," *Sensors Actuators, A Phys.*, vol. 285, pp. 50–58, Jan. 2019.

[31] D. B. Bogy and F. E. Talke, "Experimental and Theoretical Study of Wave Propagation Phenomena in Drop-on-Demand Ink Jet Devices.," *IBM J. Res. Dev.*, vol. 28, no. 3, pp. 314–321, May. 1984.

[32] J. Chang, Y. Liu, and B. Huang, "Effects of dwell time of excitation waveform on meniscus movements for a tubular piezoelectric print-head: Experiments and model," *J. Micromechanics Microengineering*, vol. 27, no. 7, Jun. 2017.

[33] Y. Zhong, H. Fang, Q. Ma, and X. Dong, "Analysis of droplet stability after ejection from an inkjet nozzle," *J. Fluid Mech.*, vol. 845, pp. 378–391, Apr. 2018.

[34] J. B. Szczech, C. M. Megaridis, D. R. Gamota, and J. Zhang, "Fine-line conductor manufacturing using drop-on-demand PZT printing technology," *IEEE Trans. Electron. Packag. Manuf.*, vol. 25, no. 1, pp. 26–33, Aug. 2002.

[35] H. Wei, X. Xiao, Z. Yin, M. Yi, and H. Zou, "A waveform design method for high DPI piezoelectric inkjet print-head based on numerical simulation," *Microsyst. Technol.*, Jan. 2017.

[36] J. Peng, J. Huang, and J. Wang, "Modelling of power-law fluid flow inside a piezoelectric inkjet printhead," *Sensors*, vol. 21, no. 7, p. 2441, Apr. 2021.

[37] J. Wang and G. T. C. Chiu, "Data-driven drop formation modeling in nanoliter drop-on-demand inkjet printing," in *ASME 2020 Dynamic Systems and Control Conference, DSCC 2020*, 2020, vol. 2.

[38] Y. Yoshida, K. Izumi, and H. Ushijima, "Nonlinear piezo-inkjet equivalent circuit modeling for predicting ink ejection velocity fluctuation caused by meniscus oscillation," *AIP Adv.*, vol. 10, no. 6, p. 065025, Jun. 2020.

[39] B. Snyder, M. Yang, S. Singhal, O. Abed, and S. V. Sreenivasan, "Automated tuning of high-order waveforms for picoliter resolution jetting of rheologically challenging materials," *Precis. Eng.*, vol. 56, pp. 143–155, Mar. 2019.

[40] H. Liu, T. Lei, C. Ma, and F. Peng, "Optimization of driven waveform of piezoelectric printhead for 3D sand-printing," *Addit. Manuf.*, vol. 37, p. 101627, Jan. 2021.

[41] P. Shin, J. Sung, and M. H. Lee, "Control of droplet formation for low viscosity fluid by double waveforms applied to a piezoelectric inkjet nozzle," *Microelectron. Reliab.*, vol. 51, no. 4, pp. 797–804, Apr. 2011.

[42] H. Y. Gan, X. Shan, T. Eriksson, B. K. Lok, and Y. C. Lam, "Reduction of droplet volume by controlling actuating waveforms in inkjet printing for micro-pattern formation," *J. Micromechanics Microengineering*, vol. 19, no. 5, Apr. 2009.

[43] Y. F. Liu, M. H. Tsai, Y. F. Pai, and W. S. Hwang, "Control of droplet formation by operating waveform for inks with various viscosities in piezoelectric inkjet printing," *Appl. Phys. A Mater. Sci. Process.*, vol. 111, no. 2, pp. 509–516, Jan. 2013.

[44] N. Morita, T. Hamazaki, and T. Ishiyama, "Observation on satellite behavior by double-pulse driving for high-speed inkjet," *J. Imaging Sci. Technol.*, vol. 60, no. 4, Jul. 2016.

[45] H. Dong, W. W. Carr, and J. F. Morris, "An experimental study of drop-on-demand drop formation," *Phys. Fluids*, vol. 18, no. 7, p. 072102, Jul. 2006.

[46] A. Fraters *et al.*, "Secondary Tail Formation and Breakup in Piezoacoustic Inkjet Printing: Femtoliter Droplets Captured in Flight," *Phys. Rev. Appl.*, vol. 13, no. 2, p. 024075, Feb. 2020.

[47] O. Oktavianty, Y. Ishii, S. Haruyama, T. Kyoutani, Z. Darmawan, and S. E. Swara, "Controlling droplet behaviour and quality of DoD inkjet printer by designing actuation waveform for multi-drop method," *IOP Conf. Ser. Mater. Sci. Eng.*, vol. 1034, no. 1, p. 012091, Feb. 2021.

[48] A. U. Chen and O. A. Basaran, "A new method for significantly reducing drop radius without reducing nozzle radius in drop-on-demand drop production," *Phys. Fluids*, vol. 14, no. 1, Dec. 2002.

[49] S. Wang, Y. Zhong, and H. Fang, "Deformation characteristics of a single droplet driven by a piezoelectric nozzle of the drop-on-demand inkjet system," *J. Fluid Mech.*, vol. 869, pp. 634–645, May. 2019.

[50] A. A. Khalate, X. Bombois, G. Scorletti, R. Babuška, S. Koekebakker, and W. De Zeeuw, "A waveform design method for a piezo inkjet printhead based on robust feedforward control," *J. Microelectromechanical Syst.*, vol. 21, no. 6, pp. 1365–1374, July. 2012.

[51] E. Dressaire and A. Sauret, "Clogging of microfluidic systems," *Soft Matter*, vol. 13, no. 1. Royal Society of Chemistry, pp. 37–48, Dec. 2017.

[52] A. Fraters *et al.*, "Inkjet Nozzle Failure by Heterogeneous Nucleation: Bubble Entrainment, Cavitation, and Diffusive Growth," *Phys. Rev. Appl.*, vol. 12, no. 6, Dec. 2019.

[53] Y. Li, O. Dahhan, C. D. M. Filipe, J. D. Brennan, and R. H. Pelton, "Optimizing piezoelectric inkjet printing of silica sols for biosensor production," *J. Sol-Gel Sci. Technol.*, vol. 87, no. 3, pp. 657–664, Sep. 2018.

[54] A. Fraters *et al.*, "Shortwave infrared imaging setup to study entrained air bubble dynamics in a MEMS-based piezo-acoustic inkjet printhead," *Exp. Fluids*, vol. 60, no. 8, p. 123, Aug. 2019.

[55] M. J. Van Der Meulen, H. Reinten, H. Wijshoff, M. Versluis, D. Lohse, and P. Steen, "Nonaxisymmetric Effects in Drop-On-Demand Piezoacoustic Inkjet Printing," *Phys. Rev. Appl.*, vol. 13, no. 5, p. 054071, May 2020.

[56] S. H. Kang, S. Kim, D. K. Sohn, and H. S. Ko, "Analysis of drop-on-demand piezo inkjet performance," *Phys. Fluids*, vol. 32, no. 2, p. 022007, Feb. 2020.

[57] U. Sen *et al.*, "The retraction of jetted slender viscoelastic liquid filaments," *physics.flu-dyn* May. 2021. DOI: arXiv:2102.08876v2.

[58] B. He, S. Yang, Z. Qin, B. Wen, and C. Zhang, "The roles of wettability and surface tension in droplet formation during inkjet printing," *Sci. Rep.*, vol. 7, no. 1, pp. 1–7, Dec. 2017.

[59] H. P. Le, "Progress and Trends in Ink-jet Printing Technology," *Journal of Imaging Science and Technology*, vol. 42, no. 1, pp. 49-62, Jan. 1998.

[60] W. Zapka, "Hewlett Packrd's Inkjet Printhead Technology, " in *Handbook of Industrial Inkjet Printing: A Full System Approach*, vol. 1&2, Wiley, 2018.

[61] J. H. Lim *et al.*, "Investigation of reliability problems in thermal inkjet printhead," in *IEEE International Reliability Physics Symposium Proceedings*, Phoenix, AZ, USA, 2004, pp. 251–254.

[62] E. Bar-Levav, M. Witman, and M. Einat, "Thin-film MEMS resistors with enhanced lifetime for thermal inkjet," *Micromachines*, vol. 11, no. 5, p. 499, May 2020.

[63] K. Shirota, M. Shioya, Y. Suga, and T. Eida, "Kogation of inorganic impurities in bubble jet ink," in *9th International Congress on Advances in Non-Impact Printing Technologies,* Yokohama, Japan. 1993. pp. 218-219.

[64] D. J. Halko, "Kogation: A New Mechanism and Solution." in *9th International Congress on Advances in Non-Impact Printing Technologies,* Yokohama, Japan. 1993. pp. 269-272.

[65] J. Park and J. Hwang, "Fabrication of a flexible Ag-grid transparent electrode using ac based electrohydrodynamic Jet printing," *J. Phys. D. Appl. Phys.*, vol. 47, no. 40, p. 405102, Sep. 2014.

[66] M. W. Lee, D. K. Kang, N. Y. Kim, H. Y. Kim, S. C. James, and S. S. Yoon, "A study of ejection modes for pulsed-DC electrohydrodynamic inkjet printing," *J. Aerosol Sci.*, vol. 46, pp. 1–6, Apr. 2012.

[67] H. T. Yudistira, V. D. Nguyen, P. Dutta, and D. Byun, "Flight behavior of charged droplets in electrohydrodynamic inkjet printing," *Appl. Phys. Lett.*, vol. 96, no. 2, p. 023503, Jan. 2010.

[68] B. W. An *et al.*, "High-Resolution Printing of 3D Structures Using an Electrohydrodynamic Inkjet with Multiple Functional Inks," *Adv. Mater.*, vol. 27, no. 29, pp. 4322–4328, Aug. 2015.

[69] C. Wei and J. Dong, "Direct fabrication of high-resolution three-dimensional polymeric scaffolds using electrohydrodynamic hot jet plotting," *J. Micromechanics Microengineering*, vol. 23, no. 2, p. 025017, Feb. 2013.

[70] S. N. Jayasinghe, M. J. Edirisinghe, and D. Z. Wang, "Controlled deposition of nanoparticle clusters by electrohydrodynamic atomization," *Nanotechnology*, vol. 15, no. 11, pp. 1519–1523, Nov. 2004.

[71] M. Kim, H. S. Yun, and G. H. Kim, "Electric-field assisted 3D-fibrous bioceramic-based scaffolds for bone tissue regeneration: Fabrication, characterization, and in vitro cellular activities," *Sci. Rep.*, vol. 7, no. 1, pp. 1–13, Dec. 2017.

[72] Y. Han and J. Dong, "High-resolution direct printing of molten-metal using electrohydrodynamic jet plotting," *Manuf. Lett.*, vol. 12, pp. 6–9, Apr. 2017.

[73] B. H. Kim *et al.*, "High-resolution patterns of quantum dots formed by electrohydrodynamic jet printing for light-emitting diodes," *Nano Lett.*, vol. 15, no. 2, pp. 969–973, Feb. 2015.

[74] D. Behera and M. Cullinan, "Current challenges and potential directions towards precision microscale additive manufacturing – Part I: Direct ink writing/jetting processes," *Precision Engineering*, vol. 68. Elsevier Inc., pp. 326–337, 01-Mar-2021.

[75] L. Y. L. Tse, "Physics-based Printhead Designs for Enhanced Electrohydrodynamic Jet Printing," *Thesis*, 2017.

[76] C. Wu *et al.*, "Electrohydrodynamic Jet Printing Driven by a Triboelectric Nanogenerator," *Adv. Funct. Mater.*, vol. 29, no. 22, p. 1901102, May 2019.

[77] E. Sutanto *et al.*, "A multimaterial electrohydrodynamic jet (E-jet) printing system," *J. Micromechanics Microengineering*, vol. 22, no. 4, p. 045008, Apr. 2012.

[78] Y. Pan, Y. A. Huang, L. Guo, Y. Ding, and Z. Yin, "Addressable multi-nozzle electrohydrodynamic jet printing with high consistency by multi-level voltage method," *AIP Adv.*, vol. 5, no. 4, p. 047108, Apr. 2015.

[79] M. F. Takagi and P. M. Ferreira, "Multi-nozzle array electrohydrodynamic jet (ejet) printing," in *Transactions of the North American Manufacturing Research Institution of SME*, Madison, WI, USA, 2013. vol. 41, pp. 548–556.

[80] K. H. Choi, K. Rahman, A. Khan, and D. S. Kim, "Cross-talk effect in electrostatic based capillary array nozzles," *J. Mech. Sci. Technol.*, vol. 25, no. 12, pp. 3053–3062, Dec. 2011.

[81] A. Khan, K. Rahman, M. T. Hyun, D. S. Kim, and K. H. Choi, "Multi-nozzle electrohydrodynamic inkjet printing of silver colloidal solution for the fabrication of electrically functional microstructures," *Appl. Phys. A Mater. Sci. Process.*, vol. 104, no. 4, pp. 1113–1120, Sep. 2011.

[82] K. H. Choi, A. Khan, K. Rahman, Y. H. Doh, D. S. Kim, and K. R. Kwan, "Effects of nozzles array configuration on cross-talk in multi-nozzle electrohydrodynamic inkjet printing head," *J. Electrostat.*, vol. 69, no. 4, pp. 380–387, Aug. 2011.

[83] S. A. Theron, A. L. Yarin, E. Zussman, and E. Kroll, "Multiple jets in electrospinning: Experiment and modeling," *Polymer (Guildf).*, vol. 46, no. 9, pp. 2889–2899, Apr. 2005.

[84] C. J. Angammana and S. H. Jayaram, "The effects of electric field on the multijet electrospinning process and fiber morphology," *IEEE Trans. Ind. Appl.*, vol. 47, no. 2, pp. 1028–1035, Mar. 2011.

[85] E. Yang, J. Shi, and Y. Xue, "Influence of electric field interference on double nozzles electrospinning," *J. Appl. Polym. Sci.*, vol. 116, no. 6, pp. 3688–3692, Jun. 2010.

[86] J. Zhang *et al.*, "Influence and evaluation of array-nozzle geometry on near- field electrospinning direct writing," *J. Eng. Fiber. Fabr.*, vol. 14, p. 155892501989564, Jan. 2019.

[87] T. H. Phung and K. S. Kwon, "How to manipulate droplet jetting from needle type jet dispensers," *Sci. Rep.*, vol. 9, no. 1, pp. 1–12, Dec. 2019.

[88] J. Jeon, S. M. Hong, M. Choi, and S. B. Choi, "Design and performance evaluation of a new jetting dispenser system using two piezostack actuators," *Smart Mater. Struct.*, vol. 24, no. 1, p. 015020, Jan. 2015.

[89] Y. Yang *et al.*, "Influence of needle impact velocity on the jetting effect of a piezoelectric needle-collision jetting dispenser," *AIP Adv.*, vol. 9, no. 4, p. 045302, Apr. 2019.

[90] M. A. Trimzi, Y. B. Ham, B. C. An, Y. M. Choi, J. H. Park, and S. N. Yun, "Development of a piezo-driven liquid jet dispenser with hinge-lever amplification mechanism," *Micromachines*, vol. 11, no. 2, p. 117, Jan. 2020.

[91] Q. H. Nguyen, S. B. Choi, and J. Do Kim, "The design and control of a jetting dispenser for semiconductor electronic packaging driven by a piezostack and a flexible beam," *Smart Mater. Struct.*, vol. 17, no. 6, p. 065028, Dec. 2008.

[92] J. W. Sohn and S. B. Choi, "Identification of operating parameters most strongly influencing the jetting performance in a piezoelectric actuator-driven dispenser," *Appl. Sci.*, vol. 8, no. 2, p. 243, Feb. 2018.

[93] W. Luo and G. Deng, "Simulation analysis of jetting dispenser based on two piezoelectric stacks," in *Proceedings - 2013 14th International Conference on Electronic Packaging Technology, ICEPT 2013*, Dilian, China, 2013, pp. 738–741.

[94] L. Wang, X. Du, Y. Li, Z. Luo, G. Zheng, and D. Sun, "Simulation and experiment study on adhesive ejection behavior in jetting dispenser," *J. Adhes. Sci. Technol.*, vol. 28, no. 1, pp. 53–64, Jan. 2014.

[95] S. Lu, G. Cao, H. Zheng, D. Li, M. Shi, and J. Qi, "Simulation and experiment on droplet formation and separation for needle-type micro-liquid jetting dispenser," *Micromachines*, vol. 9, no. 7, p. 330, Jun. 2018.

[96] X. Shan, Y. Chen, X. Peng, and H. Li, "Modeling of laminar fluid flow in jet dispensing process," in *Proceedings of the Electronic Packaging Technology Conference, EPTC*, Chengdu, China, 2014, pp. 276–279.

[97] Y. Chen, F. Wang, H. Li, and X. Shan, "Experimental and modeling study of high-viscosity silicone jet dispensing process for LED packaging," in *Proceedings of the Electronic Packaging Technology Conference, EPTC*, Chengdu, China 2014, pp. 1431–1436.

[98] C. Zhou, J. H. Li, J. A. Duan, and G. L. Deng, "The principle and physical models of novel jetting dispenser with giant magnetostrictive and a magnifier," *Sci. Rep.*, vol. 5, no. 1, p. 18294, Dec. 2015.

[99] Q. H. Nguyen, M. K. Choi, B. Y. Yun, and S. B. Choi, "Design of a novel jetting dispenser featuring piezostack and linear pump," *J. Intell. Mater. Syst. Struct.*, vol. 19, no. 3, pp. 333–341, Mar. 2008.

[100] J. Deng, "Dynamic characteristics of piezoelectric jetting dispenser with a double spring recovery system," in *IOP Conference Series: Earth and Environmental Science*, Busan, South Korea, 2021, vol. 1802, no. 4, p. 42093.

[101] Z. Bu *et al.*, "A novel piezostack-driven jetting dispenser with corner-filleted flexure hinge and high-frequency performance," *J. Micromechanics Microengineering*, vol. 28, no. 7, p. 075001, Apr. 2018.

[102] L. Wang *et al.*, "Design and experiment of a jetting dispenser with compact amplifying mechanism and low stress in piezostack," *J. Intell. Mater. Syst. Struct.*, vol. 31, no. 5, pp. 788–798, Mar. 2020.

[103] C. Zhou, J. Li, J. A. Duan, and G. Deng, "Direct-acting piezoelectric jet dispenser with rhombic mechanical amplifier," *IEEE Trans. Components, Packag. Manuf. Technol.*, vol. 8, no. 5, pp. 910–913, May 2018.

[104] X. Huang *et al.*, "Effect of enhanced squeezing needle structure on the jetting performance of a piezostack-driven dispenser," *Micromachines*, vol. 10, no. 12, p. 850, Dec. 2019.

[105] G. Deng, W. Cui, C. Zhou, and J. Li, "A piezoelectric jetting dispenser with a pin joint," *Optik (Stuttg).*, vol. 175, pp. 163–171, Dec. 2018.

[106] R. (Ross) Salary, J. P. Lombardi, D. L. Weerawarne, P. Rao, and M. D. Poliks, "A Computational Fluid Dynamics Investigation of Pneumatic Atomization, Aerosol Transport, and Deposition in Aerosol Jet Printing Process," *J. Micro Nano-Manufacturing*, vol. 9, no. 1, Mar. 2021.

[107] L. Tsui, S. C. Kayser, S. A. Strong, and J. M. Lavin, "High Resolution Aerosol Jet Printed Components with Electrodeposition-Enhanced Conductance," *ECS J. Solid State Sci. Technol.*, vol. 10, no. 4, p. 047001, Apr. 2021.

[108] C. Fisher *et al.*, "All-aerosol-jet-printed highly sensitive and selective polyaniline-based ammonia sensors: a route toward low-cost, low-power gas detection," *J. Mater. Sci.*, vol. 56, no. 22, pp. 12596–12606, Aug. 2021.

[109] Y. Zhu, L. Yu, D. Wu, W. Lv, and L. Wang, "A high-sensitivity graphene ammonia sensor via aerosol jet printing," *Sensors*

Actuators, A Phys., vol. 318, p. 112434, Feb. 2021.

[110] C. Fisher *et al.*, "All-aerosol-jet-printed highly sensitive and selective polyaniline-based ammonia sensors: a route toward low-cost, low-power gas detection," *J. Mater. Sci.*, vol. 56, no. 22, pp. 12596–12606, Aug. 2021.

[111] M. K. Hamjah, M. Steinberger, K. C. Tam, H. J. Egelhaaf, C. J. Brabec, and J. Franke, "Aerosol jet printed AgNW electrode and PEDOT:PSS layers for organic light-emitting diode devices fabrication," in *2021 14th International Congress: Molded Interconnect Devices, MID 2021 - Proceedings*, Amberg, Germany, 2021.

[112] D. Majak, J. Fan, S. Kang, and M. Gupta, "Delta-9-tetrahydrocannabinol (Δ9-THC) sensing using an aerosol jet printed organic electrochemical transistor (OECT)," *J. Mater. Chem. B*, vol. 9, no. 8, pp. 2107–2117, Feb. 2021.

[113] A. Glushkova *et al.*, "Ultrasensitive 3D Aerosol-Jet-Printed Perovskite X-ray Photodetector," *ACS Nano*, vol. 15, no. 3, pp. 4077–4084, Mar. 2021.

[114] N. J. Wilkinson, M. A. A. Smith, R. W. Kay, and R. A. Harris, "A review of aerosol jet printing—a non-traditional hybrid process for micro-manufacturing," *Int. J. Adv. Manuf. Technol.*, vol. 105, no. 11, pp. 4599–4619, Dec. 2019.

[115] A. Mahajan, C. D. Frisbie, and L. F. Francis, "Optimization of aerosol jet printing for high-resolution, high-aspect ratio silver lines," *ACS Appl. Mater. Interfaces*, vol. 5, no. 11, pp. 4856–4864, Jun. 2013.

[116] F. Vogeler, W. Verheecke, A. Voet, and H. Valkenaers, "An initial study of aerosol jet® printed interconnections on extrusion-based 3d-printed substrates," *Stroj. Vestnik/Journal Mech. Eng.*, vol. 59, no. 11, pp. 689–696, Jan. 2013.

[117] H. Zhang, J. P. Choi, S. K. Moon, and T. H. Ngo, "A knowledge transfer framework to support rapid process modeling in aerosol jet printing," *Adv. Eng. Informatics*, vol. 48, p. 101264, Apr. 2021.

[118] M. S. Brown, C. F. Brasz, Y. Ventikos, and C. B. Arnold, "Impulsively actuated jets from thin liquid films for high-resolution printing applications," *J. Fluid Mech.*, vol. 709, pp. 341–370, Aug. 2012.

[119] V. Keriquel *et al.*, "In situ printing of mesenchymal stromal cells, by laser-assisted bioprinting, for in vivo bone regeneration applications," *Sci. Rep.*, vol. 7, no. 1, pp. 1–10, Dec. 2017.

[120] O. A. Abbas *et al.*, "Laser printed two-dimensional transition metal dichalcogenides," *Sci. Rep.*, vol. 11, no. 1, p. 5211, Dec. 2021.

[121] P. Delrot, M. A. Modestino, F. Gallaire, D. Psaltis, and C. Moser, "Inkjet Printing of Viscous Monodisperse Microdroplets by Laser-Induced Flow Focusing," *Phys. Rev. Appl.*, vol. 6, no. 2, p. 024003, Aug. 2016.

[122] I. Theodorakos *et al.*, "Laser-Induced Forward Transfer of High Viscous, Non-Newtonian Silver Nanoparticle Inks: Jet Dynamics and Temporal Evolution of the Printed Droplet Study," *Adv. Eng. Mater.*, vol. 21, no. 10, July. 2019.

[123] M. Makrygianni, A. Millionis, C. Kryou, I. Trantakis, D. Poulikakos, and I. Zergioti, "On-Demand Laser Printing of Picoliter-Sized, Highly Viscous, Adhesive Fluids: Beyond Inkjet Limitations," *Adv. Mater. Interfaces*, vol. 5, no. 18, p. 1800440, Sep. 2018.

[124] J. Jang, H. G. Yi, and D. W. Cho, "3D Printed Tissue Models: Present and Future," *ACS Biomaterials Science and Engineering*, vol. 2, no. 10. American Chemical Society, pp. 1722–1731, Oct. 2016.

[125] S. A. Elrod *et al.*, "Nozzleless droplet formation with focused acoustic beams," *J. Appl. Phys.*, vol. 65, no. 9, pp. 3441–3447, Jan. 1989.

[126] B. Hadimioglu *et al.*, "Acoustic ink printing," in *Proceedings - IEEE Ultrasonics Symposium*, Tucson, AZ, USA, 1992, pp. 929–935.

[127] Q. Guo, X. Su, X. Zhang, M. Shao, H. Yu, and D. Li, "A review on acoustic droplet ejection technology and system," *Soft Matter*, vol. 17, no. 11. Royal Society of Chemistry, pp. 3010–3021, Mar. 2021.

[128] S. Jentsch, R. Nasehi, C. Kuckelkorn, B. Gundert, S. Aveic, and H. Fischer, "Multiscale 3D Bioprinting by Nozzle-Free Acoustic Droplet Ejection," *Small Methods*, vol. 5, no. 6, p. 2000971, Jun. 2021.

[129] Y. Lei and H. Hu, "SAW-driven droplet jetting technology in microfluidic: A review," *Biomicrofluidics*, vol. 14, no. 6. Dec. 2020.

[130] J. K., Y. Q., and W. I., "Acoustic Wave Based Microfluidics and Lab-on-a-Chip," in *Modeling and Measurement Methods for Acoustic Waves and for Acoustic Microdevices*, Aug. 2013.

[131] M. K. Tan, J. R. Friend, and L. Y. Yeo, "Interfacial Jetting Phenomena Induced by Focused Surface Vibrations," *Phys. Rev. Lett.*, vol. 103, no. 2, July. 2009.

[132] M. H. Biroun, M. Rahmati, M. Jangi, B. Chen, and Y. Q. Fu, "Numerical and experimental investigations of interdigital transducer configurations for efficient droplet streaming and jetting induced by surface acoustic waves," *Int. J. Multiph. Flow*, vol. 136, Mar. 2021.

[133] J. O. Castro, S. Ramesan, A. R. Rezk, and L. Y. Yeo, "Continuous tuneable droplet ejection via pulsed surface acoustic wave jetting," *Soft Matter*, vol. 14, no. 28, pp. 5721–5727, Mar. 2018.

[134] T. Dung Luong and N. Trung Nguyen, "Surface Acoustic Wave Driven Microfluidics – A Review," *Micro Nanosyst.*, vol. 2, no. 3, pp. 217–225, Sept. 2010.

[135] N. Jackson, W. Voit, R. Trip, A. Condie, and X. Plc, "Jetting Very High Viscosities With Piezo-Electric Drop-On-Demand Printheads For Increased Capability Of Photopolymer 3D Printing," *NIP Digit. Fabr. Conf.*, vol. 2019, no. 1, pp. 89–93, 2019.

[136] T. T. T. Can, T. C. Nguyen, and W. S. Choi, "Patterning of High-Viscosity Silver Paste by an Electrohydrodynamic-Jet Printer for Use in TFT Applications," *Sci. Rep.*, vol. 9, no. 1, Jun. 2019.

[137] J. A. Lewis, "Direct ink writing of 3D functional materials," *Adv. Funct. Mater.*, vol. 16, no. 17, pp. 2193–2204, Oct. 2006.

[138] D. K. Kang, M. W. Lee, H. Y. Kim, S. C. James, and S. S. Yoon, "Electrohydrodynamic pulsed-inkjet characteristics of various inks containing aluminum particles," *J. Aerosol Sci.*, vol. 42, no. 10, pp. 621–630, Oct. 2011.

[139] T. T. T. Can, T. C. Nguyen, and W. S. Choi, "High-Viscosity Copper Paste Patterning and Application to Thin-Film

Transistors Using Electrohydrodynamic Jet Printing," *Adv. Eng. Mater.*, vol. 22, no. 3, Jan. 2020.

[140] R. Houben, "Equipment for printing of High Viscosity Liquids and Molten Metals," Ph.D. dissertation, Dept. TNO, Phy. of Fluid, Univ. of Twentee, Enschede, Netherlands, 2012.

[141] Z. Zhang, R. Xiong, R. Mei, Y. Huang, and D. B. Chrisey, "Time-Resolved Imaging Study of Jetting Dynamics during Laser Printing of Viscoelastic Alginate Solutions," *Langmuir*, vol. 31, no. 23, pp. 6447–6456, May. 2015.

[142] Q. H. Nguyen, M. K. Choi, and S. B. Choi, "A new type of piezostack-driven jetting dispenser for semiconductor electronic packaging: Modeling and control," *Smart Mater. Struct.*, vol. 17, no. 1, Jan. 2008.

[143] S. Lu, G. Cao, H. Zheng, D. Li, M. Shi, and J. Qi, "Simulation and experiment on droplet formation and separation for needle-type micro-liquid jetting dispenser," *Micromachines*, vol. 9, no. 7, Jun. 2018.

[144] S. Lu *et al.*, "Nozzle and needle during high viscosity adhesive jetting based on piezoelectric jet dispensing," *Smart Mater. Struct.*, vol. 24, no. 10, 2015.

[145] L. Wang *et al.*, "Design and experiment of a jetting dispenser driven by piezostack actuator," *IEEE Trans. Components, Packag. Manuf. Technol.*, vol. 3, no. 1, pp. 147–156, Jan. 2013.

[146] B. H. King and M. J. Renn, "Aerosol Jet® Direct Write Printing for Mil-Aero Electronic Applications," Optomec Inc, 2009.

[147] M. Bevione and A. Chiolerio, "Benchmarking of Inkjet Printing Methods for Combined Throughput and Performance," *Adv. Eng. Mater.*, vol. 22, no. 12, p. 2000679, Dec. 2020.

[148] V. Beedasy and P. J. Smith, "Printed electronics as prepared by inkjet printing," *Materials*, vol. 13, no. 3. 2020.

[149] M. Hartwig, R. Zichner, and Y. Joseph, "Inkjet-printed wireless chemiresistive sensors-A review," *Chemosensors*, vol. 6, no. 4. 2018.

[150] A. Sajedi-Moghaddam, E. Rahmanian, and N. Naseri, "Inkjet-printing technology for supercapacitor application: Current state and perspectives," *ACS Appl. Mater. Interfaces*, vol. 12, no. 31, pp. 34487–34504, 2020.

[151] S. Kholghi Eshkalak, A. Chinnappan, W. A. D. M. Jayathilaka, M. Khatibzadeh, E. Kowsari, and S. Ramakrishna, "A review on inkjet printing of CNT composites for smart applications," *Applied Materials Today*, vol. 9. pp. 372–386, 2017.

[152] N. Scoutaris, S. Ross, and D. Douroumis, "Current Trends on Medical and Pharmaceutical Applications of Inkjet Printing Technology," *Pharmaceutical Research*, vol. 33, no. 8. pp. 1799–1816, 2016.

[153] R. Daly, T. S. Harrington, G. D. Martin, and I. M. Hutchings, "Inkjet printing for pharmaceutics - A review of research and manufacturing," *Int. J. Pharm.*, vol. 494, no. 2, pp. 554–567, Oct. 2015.

[154] G. Cummins and M. P. Y. Desmulliez, "Inkjet printing of conductive materials: A review," *Circuit World*, vol. 38, no. 4. pp. 193–213, Nov. 2012.

[155] A. Briggs-Goode and A. Russell, "Printed textile design," in *Textile Design*, Elsevier, 2011, pp. 105-129e.

[156] H. Ujiie, *"Digital Printing of Textiles,"* CRC press, Boca Raton, FL, USA, 2006.

[157] T. C. de Goede, K. G. de Bruin, N. Shahidzadeh, and D. Bonn, "Droplet Splashing on Rough Surfaces," *Phys. Rev. Fluids*, vol. 6, no. 4, p. 043604, Apr. 2021.

[158] M. Marengo, C. Antonini, I. V. Roisman, and C. Tropea, "Drop collisions with simple and complex surfaces," *Current Opinion in Colloid and Interface Science*, vol. 16, no. 4. Elsevier, pp. 292–302, Aug. 2011.

[159] C. Josserand and S. T. Thoroddsen, "Drop Impact on a Solid Surface," *Annu. Rev. Fluid Mech.*, vol. 48, no. 1, pp. 365–391, Jan. 2016.

[160] M. Rein, "Phenomena of liquid drop impact on solid and liquid surfaces," *Fluid Dyn. Res.*, vol. 12, no. 2, pp. 61–93, Aug. 1993.

[161] A. L. Yarin, "Drop impact dynamics: Splashing, spreading, receding, bouncing..," *Annu. Rev. Fluid Mech.*, vol. 38, no. 1, pp. 159–192, Jan. 2006.

[162] D. Khojasteh, M. Kazerooni, S. Salarian, and R. Kamali, "Droplet impact on superhydrophobic surfaces: A review of recent developments," *Journal of Industrial and Engineering Chemistry*, vol. 42. Korean Society of Industrial Engineering Chemistry, pp. 1–14, Oct. 2016.

[163] K. Zhang *et al.*, "The effect of ink drop spreading and coalescing on the image quality of printed cotton fabric," *Cellulose*, vol. 27, no. 16, pp. 9725–9736, Nov. 2020.

[164] G. Zhang, M. A. Quetzeri-Santiago, C. A. Stone, L. Botto, and J. R. Castrejón-Pita, "Droplet impact dynamics on textiles," *Soft Matter*, vol. 14, no. 40, pp. 8182–8190, Oct. 2018.

[165] T. C. De Goede *et al.*, "Droplet impact of Newtonian fluids and blood on simple fabrics: Effect of fabric pore size and underlying substrate," *Phys. Fluids*, vol. 33, no. 3, p. 33308, Mar. 2021.

[166] C. Fairhurst, "Advances in Apparel Production," CRC press, Boca Raton, FL, USA, 2008.

[167] Y. Ding, R. Shamey, L. P. Chapman, and H. S. Freeman, "Pretreatment effects on pigment-based textile inkjet printing – colour gamut and crockfastness properties," *Color. Technol.*, vol. 135, no. 1, pp. 77–86, Feb. 2019.

[168] H. J. Kim, J. P. Hong, D. S. Kwak, and D. J. Kwon, "Acrylic polymer treatment on Nylon fibers improves color strength and durability in thermal transfer printing," *Colloids Surfaces A Physicochem. Eng. Asp.*, vol. 615, p. 126268, Apr. 2021.

[169] C. Li *et al.*, "Synergistic Effects of Alpha Olefin Sulfonate and Sodium Alginate on Inkjet Printing of Cotton/Polyamide Fabrics," *Langmuir*, vol. 37, no. 2, pp. 683–692, Jan. 2021.

[170] T. Biswas, J. Yu, and V. Nierstrasz, "Effective Pretreatment Routes of Polyethylene Terephthalate Fabric for Digital Inkjet Printing of Enzyme," *Adv. Mater. Interfaces*, vol. 8, no. 6, p. 2001882, Mar. 2021.

[171] F. An, K. Fang, X. Liu, H. Yang, and G. Qu, "Protease and sodium alginate combined treatment of wool fabric for enhancing inkjet printing performance of reactive dyes," *Int. J. Biol. Macromol.*, vol. 146, pp. 959–964, Mar. 2020.

[172] Y. Song, K. Fang, M. N. Bukhari, Y. Ren, K. Zhang, and Z. Tang, "Green and Efficient Inkjet Printing of Cotton Fabrics

Using Reactive Dye@Copolymer Nanospheres," *ACS Appl. Mater. Interfaces*, vol. 12, no. 40, pp. 45281–45295, Oct. 2020.

[173] H. Qin, K. Fang, Y. Ren, K. Zhang, L. Zhang, and X. Zhang, "Insights into influences of dye hydrophobicity on cleanliness and resolution of fabric ink-jet printing," *ACS Sustain. Chem. Eng.*, vol. 8, no. 46, pp. 17291–17298, Nov. 2020.

[174] C. Gao, T. Xing, X. Hou, Y. Zhang, and G. Chen, "Clean production of polyester fabric inkjet printing process without fabric pretreatment and soaping," *J. Clean. Prod.*, vol. 282, p. 124315, Feb. 2021.

[175] Y. Ding, W. Zhendong, Z. Chuanxiong, X. Ruobai, and X. Wenliang, "A study on the applicability of pigment digital printing on cotton fabrics," *Text. Res. J.*, Mar. 2021.

[176] B. Gooby, " The Development of Methodologies for Color Printing in Digital Inkjet Textile Printing and the Application of Color Knowledge in the Ways of Making Project ," *J. Text. Des. Res. Pract.*, vol. 8, no. 3, pp. 358–383, Sep. 2020.

[177] X. Zhang, K. Fang, H. Zhou, K. Zhang, and M. N. Bukhari, "Enhancing inkjet image quality through controlling the interaction of complex dye and diol molecules," *J. Mol. Liq.*, vol. 312, p. 113481, Aug. 2020.

[178] T. Tofan, R. Stonkus, and R. Jasevičius, "Investigation of color reproduction on linen fabrics when printing with mimaki tx400-1800d inkjet with pigment tp250 dyes," *Coatings*, vol. 11, no. 3, p. 354, Mar. 2021.

[179] K. Chatterjee and T. K. Ghosh, "3D Printing of Textiles: Potential Roadmap to Printing with Fibers," *Advanced Materials*, vol. 32, no. 4. Wiley-VCH Verlag, p. 1902086, Jan. 2020.

[180] Y. Huang, E. L. Hsiang, M. Y. Deng, and S. T. Wu, "Mini-LED, Micro-LED and OLED displays: present status and future perspectives," *Light: Science and Applications*, vol. 9, no. 1. Springer Nature, pp. 2047–7538, Dec. 2020.

[181] S. M. Lee, J. H. Kwon, S. Kwon, and K. C. Choi, "A Review of Flexible OLEDs Toward Highly Durable Unusual Displays," *IEEE Transactions on Electron Devices*, vol. 64, no. 5. Institute of Electrical and Electronics Engineers Inc., pp. 1922–1931, May. 2017.

[182] L. Ma and Y. fei Shao, "A brief review of innovative strategies towards structure design of practical electronic display device," *Journal of Central South University*, vol. 27, no. 6. Central South University of Technology, pp. 1624–1644, Jun. 2020.

[183] X. Zheng *et al.*, "Efficient inkjet-printed blue OLED with boosted charge transport using host doping for application in pixelated display," *Opt. Mater. (Amst).*, vol. 101, p. 109755, Mar. 2020.

[184] D. G. Yoon, Y. J. Kang, R. Bail, and B. D. Chin, "Interfaces and pattern resolution of inkjet-printed organic light-emitting diodes with a novel hole transport layer," *J. Inf. Disp.*, vol. 2021, no. 2, pp. 91–98, Jan. 2021.

[185] T. Zhaobing, M. Linjia, S. Mingxiao, K. Namdeog, and L. Weidong, "54.2: Preparation of inkjet printing organic light-emitting diode by optimizing the formation of flat film," *SID Symp. Dig. Tech. Pap.*, vol. 52, no. S1, pp. 392–394, Feb. 2021.

[186] C. Feng *et al.*, "Highly efficient inkjet printed flexible organic light-emitting diodes with hybrid hole injection layer," *Org. Electron.*, vol. 85, p. 105822, Oct. 2020.

[187] X. Cao, Y. Ye, X. Liu, T. Guo, and Q. Tang, "54.3: Realization of Uniform OLED Pixels based on Multi-nozzle by Inkjet printing," *SID Symp. Dig. Tech. Pap.*, vol. 52, no. S1, pp. 395–397, Feb. 2021.

[188] C. Amruth, B. Luszczynska, W. Rekab, M. Z. Szymanski, and J. Ulanski, "Inkjet printing of an electron injection layer: New role of cesium carbonate interlayer in polymer oleds," *Polymers (Basel).*, vol. 13, no. 1, pp. 1–16, Dec. 2021.

[189] W. Deferme, M. Cramer, J. Drijkoningen, and I. Verboven, "Optimizing the outcoupling efficiency and the radiation pattern of organic light emitting devices by inkjet printing lens arrays films," 2018, vol. 10687, p. 34.

[190] I. Sachs, M. Fuhrmann, I. Verboven, I. Basak, W. Deferme, and H. Möbius, "Inkjet Printed Lenses with Adjustable Contact Angle to Improve the Light Out-Coupling of Organic Light Emitting Diodes," *Adv. Eng. Mater.*, p. adem.202100212, Apr. 2021.

[191] Z. Gao *et al.*, " 47.2: Invited Paper: 31 inch Rollable OLED Display Fabricated by Inkjet Printing Technology ," *SID Symp. Dig. Tech. Pap.*, vol. 52, no. S1, pp. 312–314, Feb. 2021.

[192] Z. Wu *et al.*, "Development of 55inch 8k amoled tv by inkjet printing process," in *Digest of Technical Papers - SID International Symposium*, 2020, vol. 51, no. 1, pp. 481–484.

[193] Y. Sun, Y. Jiang, X. W. Sun, S. Zhang, and S. Chen, "Beyond OLED: Efficient Quantum Dot Light-Emitting Diodes for Display and Lighting Application," *Chemical Record*, vol. 19, no. 8. John Wiley and Sons Inc, pp. 1729–1752, 01-Aug-2019.

[194] Z. Liu *et al.*, "Micro-light-emitting diodes with quantum dots in display technology," *Light: Science and Applications*, vol. 9, no. 1. Springer Nature, pp. 2047–7538, 01-Dec-2020.

[195] J. H. Kim, Y. J. Kang, and B. D. Chin, "Solvent mixture formulation for orthogonal inkjet processing and uniform pixel patterning of quantum dot light-emitting diode," *J. Korean Phys. Soc.*, pp. 1–12, May 2021.

[196] M. Chen *et al.*, "High performance inkjet-printed QLEDs with 18.3% EQE: improving interfacial contact by novel halogen-free binary solvent system," *Nano Res.*, pp. 1–7, Feb. 2021.

[197] Y. Lin, Y.-W. Chang, B.-R. Hyun, C.-W. Sher, H.-C. Kuo, and Z. Liu, "P-12.2: Inkjet-printed Quantum-dots Photopolymers for Full-color Micro-LED Displays," *SID Symp. Dig. Tech. Pap.*, vol. 52, no. S1, pp. 597–600, Feb. 2021.

[198] Z. Hu *et al.*, "Inkjet printed uniform quantum dots as color conversion layers for full-color OLED displays," *Nanoscale*, vol. 12, no. 3, pp. 2103–2110, Jan. 2020.

[199] H. C. Wang, Z. Bao, H. Y. Tsai, A. C. Tang, and R. S. Liu, "Perovskite Quantum Dots and Their Application in Light-Emitting Diodes," *Small*, vol. 14, no. 1. Wiley-VCH Verlag, p. 1702433, Jan. 2018.

[200] S. Shi, W. Bai, T. Xuan, T. Zhou, G. Dong, and R. J. Xie, "In Situ Inkjet Printing Patterned Lead Halide Perovskite Quantum Dot Color Conversion Films by Using Cheap and Eco-Friendly Aqueous Inks," *Small Methods*, vol. 5, no. 3, p. 2000889, Mar. 2021.

[201] J. H. Yoo, S. G. Jeong, S. H. Choi, S. Bin Kwon, Y. H. Song, and D. H. Yoon, "Drying stability enhancement of red-

perovskite colloidal ink via ligand-derived coating for inkjet printing," *Ceram. Int.*, vol. 47, no. 5, pp. 6041–6048, Mar. 2021.

[202] S. Y. Lee *et al.*, "Investigation of high-performance perovskite nanocrystals for inkjet-printed color conversion layers with superior color purity," *APL Photonics*, vol. 6, no. 5, p. 056104, May 2021.

[203] C. Zheng *et al.*, "High-brightness perovskite quantum dot light-emitting devices using inkjet printing," *Org. Electron.*, vol. 93, p. 106168, Jun. 2021.

[204] D. Wallace *et al.*, "Ink-jet as a MEMS manufacturing tool," in *Proceedings of the International Conference on Integration and Commercialization of Micro and Nanosystems 2007*, 2007, vol. B, pp. 1161–1168.

[205] G. Percin, T. H. Soh, and B. T. Khuri-Yakub, "Resist deposition without spinning by using novel inkjet technology and direct lithography for MEMS," in *Advances in Resist Technology and Processing XV*, 1998, vol. 3333, p. 1382.

[206] G. Perçin and B. T. Khuri-Yakub, "Photoresist deposition without spinning," *IEEE Trans. Semicond. Manuf.*, vol. 16, no. 3, pp. 452–459, 2003.

[207] A. Bietsch, M. Hegner, H. P. Lang, and C. Gerber, "Inkjet deposition of alkanethiolate monolayers and DNA oligonucleotides on gold: Evaluation of spot uniformity by wet etching," *Langmuir*, vol. 20, no. 12, pp. 5119–5122, 2004.

[208] T. Fukushima, K. Nishio, and H. Masuda, "Inkjet printing for site-controlled tunnel pitting with high aspect ratio in al," *Electrochem. Solid-State Lett.*, vol. 13, no. 4, 2010.

[209] X. Qu, J. Li, Z. Yin, and H. Zou, "New lithography technique based on electrohydrodynamic printing platform," *Org. Electron.*, vol. 71, pp. 279–283, 2019.

[210] R. Bernasconi, M. C. Angeli, F. Mantica, D. Carniani, and L. Magagnin, "SU-8 inkjet patterning for microfabrication," *Polymer (Guildf).*, vol. 185, p. 121933, Dec. 2019.

[211] R. Danzebrink and M. A. Aegerter, "Deposition of micropatterned coating using an ink-jet technique," *Thin Solid Films*, vol. 351, no. 1–2, pp. 115–118, 1999.

[212] R. Danzebrink and M. A. Aegerter, "Deposition of optical microlens arrays by ink-jet processes," in *Thin Solid Films*, 2001, vol. 392, no. 2, pp. 223–225.

[213] V. J. Cadarso *et al.*, "Microlenses with defined contour shapes," *Opt. Express*, vol. 19, no. 19, p. 18665, 2011.

[214] L. Jacot-Descombes, M. R. Gullo, V. J. Cadarso, and J. Brugger, "Fabrication of epoxy spherical microstructures by controlled drop-on-demand inkjet printing," *J. Micromechanics Microengineering*, vol. 22, no. 7, 2012.

[215] X. Zhu, L. Zhu, H. Chen, M. Yang, and W. Zhang, "Fabrication of multi-scale micro-lens arrays on hydrophobic surfaces using a drop-on-demand droplet generator," *Opt. Laser Technol.*, vol. 66, pp. 156–165, 2015.

[216] J. Y. Kim, K. Pfeiffer, A. Voigt, G. Gruetzner, and J. Brugger, "Directly fabricated multi-scale microlens arrays on a hydrophobic flat surface by a simple ink-jet printing technique," *J. Mater. Chem.*, vol. 22, no. 7, pp. 3053–3058, 2012.

[217] J. Y. Kim, C. Martin-Olmos, N. S. Baek, and J. Brugger, "Simple and easily controllable parabolic-shaped microlenses printed on polymeric mesas," *J. Mater. Chem. C*, vol. 1, no. 11, pp. 2152–2157, Jan. 2013.

[218] Y. Luo *et al.*, "Direct fabrication of microlens arrays with high numerical aperture by ink-jetting on nanotextured surface," *Appl. Surf. Sci.*, vol. 279, pp. 36–40, Aug. 2013.

[219] A. J. Lennon, A. W. Y. Ho-Baillie, and S. R. Wenham, "Direct patterned etching of silicon dioxide and silicon nitride dielectric layers by inkjet printing," *Sol. Energy Mater. Sol. Cells*, vol. 93, no. 10, pp. 1865–1874, Oct. 2009.

[220] I. A. Grimaldi, A. De Girolamo Del Mauro, G. Nenna, F. Loffredo, C. Minarini, and F. Villani, "Inkjet etching of polymer surfaces to manufacture microstructures for OLED applications," in *AIP Conference Proceedings*, 2010, vol. 1255, pp. 104–106.

[221] I. A. Grimaldi, A. De Girolamo Del Mauro, G. Nenna, F. Loffredo, C. Minarini, and F. Villani, "Microstructuring of polymer films by inkjet etching," in *Journal of Applied Polymer Science*, vol. 122, no. 6, pp. 3637–3643, Aug. 2011.

[222] W. H. Lee and Y. D. Park, "Inkjet etching of polymers and its applications in organic electronic devices," *Polymers*. Sep. 2017.

[223] S. Chung, K. Cho, and T. Lee, "Recent Progress in Inkjet-Printed Thin-Film Transistors," *Advanced Science*, vol. 6, no. 6. Jan. 2019.

[224] J. Kim, B. J. Ahn, D. Chae, J. Shin, W. H. Lee, and S. Ko, "Silver film etching processing using the inkjet method for the organic thin film transistor," *Org. Electron.*, Feb. 2019.

[225] Y. Li *et al.*, "All Inkjet-Printed Metal-Oxide Thin-Film Transistor Array with Good Stability and Uniformity Using Surface-Energy Patterns," *ACS Appl. Mater. Interfaces*, vol. 9, no. 9, pp. 8194–8200, Feb. 2017.

[226] G. K. Lau and M. Shrestha, "Ink-jet printing of micro-elelectro-mechanical systems (MEMS)," *Micromachines*, vol. 8, no. 6, Jun. 2017.

[227] D. Kuscer, O. Noshchenko, H. Uršič, and B. Malič, "Piezoelectric properties of ink-jet-printed lead zirconate titanate thick films confirmed by piezoresponse force microscopy," *J. Am. Ceram. Soc.*, vol. 96, no. 9, pp. 2714–2717, Aug. 2013.

[228] D. Kuscer, S. Drnovšek, and F. Levassort, "Inkjet-printing-derived lead-zirconate-titanate-based thick films for printed electronics," *Mater. Des.*, vol. 198, p. 109324, Jan. 2021.

[229] N. Godard, S. Glinšek, A. Matavž, V. Bobnar, and E. Defay, "Direct Patterning of Piezoelectric Thin Films by Inkjet Printing," *Adv. Mater. Technol.*, vol. 4, no. 2, 2019.

[230] N. Godard, M. A. Mahjoub, S. Girod, T. Schenk, S. Glinšek, and E. Defay, "On the importance of pyrolysis for inkjet-printed oxide piezoelectric thin films," *J. Mater. Chem. C*, vol. 8, no. 11, pp. 3740–3747, Jan. 2020.

[231] O. Pabst *et al.*, "Inkjet printed micropump actuator based on piezoelectric polymers: Device performance and morphology studies," *Org. Electron.*, vol. 15, no. 11, pp. 3306–3315, Nov. 2014.

[232] F. Zheng, Z. Wang, J. Huang, and Z. Li, "Inkjet printing-based fabrication of microscale 3D ice structures," *Microsystems Nanoeng.*, vol. 6, no. 1, pp. 1–10, Dec. 2020.

[233] F. Zheng, J. Huang, and Z. Li, "Fabrication of 3D Micro Ice

Structures Based on Inkjet Printing," in *Proceedings of the IEEE International Conference on Micro Electro Mechanical Systems (MEMS)*, Seoul, South Korea, 2019, pp. 368–371.

[234] N. Godard, S. Glinsek, and E. Defay, "Inkjet-printed silver as alternative top electrode for lead zirconate titanate thin films," *J. Alloys Compd.*, vol. 783, pp. 801–805, Apr. 2019.

[235] S. B. Fuller, E. J. Wilhelm, and J. M. Jacobson, "Ink-jet printed nanoparticle microelectromechanical systems," *J. Microelectromechanical Syst.*, vol. 11, no. 1, pp. 54–60, Feb. 2002.

[236] S. Sollami Delekta, K. H. Adolfsson, N. Benyahia Erdal, M. Hakkarainen, M. Östling, and J. Li, "Fully inkjet printed ultrathin microsupercapacitors based on graphene electrodes and a nano-graphene oxide electrolyte," *Nanoscale*, vol. 11, no. 21, pp. 10172–10177, Jun. 2019.

[237] A. Kaneko, A. Mori, K. Kanada, C. Sumin, and W. Ke, "Micro/Nano-Printing of Metal and Nanoparticle Thin Film and its Application to MEMS Device," in *JSME 2020 Conference on Leading Edge Manufacturing/Materials and Processing,* 2020.

[238] D. J. Hayes, W. R. Cox, and D. B. Wallace, "Printing systems for MEMS packaging," in *Reliability, Testing, and Characterization of MEMS/MOEMS*, San Francisco, CA, USA, 2001, vol. 4558, pp. 206–214.

[239] B. Khorramdel and M. Mäntysalo, "Inkjet filling of TSVs with silver nanoparticle ink," in *Proceedings of the 5th Electronics System-Integration Technology Conference, ESTC 2014*, Helsinki, Finland, 2014.

[240] B. Khorramdel and M. Mäntysalo, "Fabrication and electrical characterization of partially metallized vias fabricated by inkjet," *J. Micromechanics Microengineering*, vol. 26, no. 4, p. 045017, Mar. 2016.

[241] N. Quack, J. Sadie, V. Subramanian, and M. C. Wu, "Through Silicon Vias and thermocompression bonding using inkjet-printed gold nanoparticles for heterogeneous MEMS integration," in *2013 Transducers and Eurosensors XXVII: The 17th International Conference on Solid-State Sensors, Actuators and Microsystems, TRANSDUCERS and EUROSENSORS 2013*, Barcelona, Spain, 2013, pp. 834–837.

[242] T. H. Yang, Z. L. Guo, Y. M. Fu, Y. T. Cheng, Y. F. Song, and P. W. Wu, "A low temperature inkjet printing and filling process for low resistive silver TSV fabrication in a SU-8 substrate," in *Proceedings of the IEEE International Conference on Micro Electro Mechanical Systems (MEMS)*, Las Vegas, NV, USA, 2017, pp. 749–752.

[243] J. H. Yang, K. L. Tsou, Y. M. Fu, Y. T. Cheng, and Y. F. Song, "Process Development of Low Resistive Ag-Based Through Silicon Vias using Inkjet Printing Technique for 3D Microsystem Integration," in *Proceedings of the IEEE International Conference on Micro Electro Mechanical Systems (MEMS)*, Seoul, South Korea, 2019, pp. 376–379.

[244] B. Khorramdel *et al.*, "Inkjet printing technology for increasing the i/o density of 3d tsv interposers," *Microsystems Nanoeng.*, vol. 3, no. 1, pp. 1–9, Apr. 2017.

[245] A. Roshanghias *et al.*, "The Realization of Redistribution Layers for FOWLP by Inkjet Printing," *Proceedings*, vol. 2, no. 13, p. 703, Dec. 2018.

[246] A. Roshanghias *et al.*, "On the feasibility of fan-out wafer-level packaging of capacitive micromachined ultrasound transducers (CMUT) by using inkjet-printed redistribution layers," *Micromachines*, vol. 11, no. 6, p. 564, May 2020.

[247] A. Roshanghias, M. Krivec, and A. Binder, "Digital micro-dispension of non-conductive adhesives (NCA) by inkjet printer," in *2017 IEEE 19th Electronics Packaging Technology Conference, EPTC 2017*, Singapore, 2018, pp. 1–3.

[248] A. Roshanghias, Y. Ma, E. Gaumont, and L. Neumaier, "Inkjet printed adhesives for advanced M(O)EMS packaging," *J. Mater. Sci. Mater. Electron.*, vol. 30, no. 22, pp. 20285–20291, Nov. 2019.

[249] K. Sakuma, "Flexible, Wearable, and Stretchable Electronics, " 1st ed, CRC press, 2020.

[250] Y. Gu *et al.*, "Mini Review on Flexible and Wearable Electronics for Monitoring Human Health Information," *Nanoscale Research Letters*, vol. 14, no. 1. Springer New York LLC, p. 263, Dec. 2019.

[251] A. Al-Halhouli, H. Qitouqa, A. Alashqar, and J. Abu-Khalaf, "Inkjet printing for the fabrication of flexible/stretchable wearable electronic devices and sensors," *Sensor Review*, vol. 38, no. 4. Emerald Group Publishing Ltd., pp. 438–452, Sep. 2018.

[252] I. Kim, J. S. Heo, and M. F. Hossain, "Challenges in design and fabrication of flexible/stretchable carbon-and textile-based wearable sensors for health monitoring: A critical review," *Sensors (Switzerland)*, vol. 20, no. 14, pp. 1–29, Jul. 2020.

[253] Q. Huang, K. N. Al-Milaji, and H. Zhao, "Inkjet Printing of Silver Nanowires for Stretchable Heaters," *ACS Appl. Nano Mater.*, vol. 1, no. 9, pp. 4528–4536, Sep. 2018.

[254] J. Abu-Khalaf, R. Saraireh, S. Eisa, and A. Al-Halhouli, "Experimental characterization of inkjet-printed stretchable circuits for wearable sensor applications," *Sensors (Switzerland)*, vol. 18, no. 10, p. 3476, Oct. 2018.

[255] Z. Cui, Y. Han, Q. Huang, J. Dong, and Y. Zhu, "Electrohydrodynamic printing of silver nanowires for flexible and stretchable electronics," *Nanoscale*, vol. 10, no. 15, pp. 6806–6811, Apr. 2018.

[256] M. Tavakoli *et al.*, "EGaIn-Assisted Room-Temperature Sintering of Silver Nanoparticles for Stretchable, Inkjet-Printed, Thin-Film Electronics," *Adv. Mater.*, vol. 30, no. 29, p. 1801852, Jul. 2018.

[257] E. Kuusisto, J. J. Heikkinen, P. Järvinen, T. Sikanen, S. Franssila, and V. Jokinen, "Inkjet-printed flexible silver electrodes on thiol-enes," *Sensors Actuators, B Chem.*, vol. 336, p. 129727, Jun. 2021.

[258] R. Mikkonen, P. Puistola, I. Jönkkäri, and M. Mäntysalo, "Inkjet Printable Polydimethylsiloxane for All-Inkjet-Printed Multilayered Soft Electrical Applications," *ACS Appl. Mater. Interfaces*, vol. 12, no. 10, pp. 11990–11997, Mar. 2020.

[259] C. T. Wang, K. Y. Huang, D. T. W. Lin, W. C. Liao, H. W. Lin, and Y. C. Hu, "A flexible proximity sensor fully fabricated by inkjet printing," *Sensors*, vol. 10, no. 5, pp. 5054–5062, May 2010.

[260] N. Karim, S. Afroj, S. Tan, K. S. Novoselov, and S. G. Yeates, "All Inkjet-Printed Graphene-Silver Composite Ink on Textiles for Highly Conductive Wearable Electronics Applications," *Sci. Rep.*, vol. 9, no. 1, pp. 1–10, Dec. 2019.

[261] B. A. Kuzubasoglu, E. Sayar, C. Cochrane, V. Koncar, and S. K. Bahadir, "Wearable temperature sensor for human body temperature detection," *J. Mater. Sci. Mater. Electron.*, vol. 32, no. 4, pp. 4784–4797, Feb. 2021.

[262] T. Vuorinen, J. Niittynen, T. Kankkunen, T. M. Kraft, and M. Mäntysalo, "Inkjet-printed graphene/PEDOT:PSS temperature sensors on a skin-conformable polyurethane substrate," *Sci. Rep.*, vol. 6, no. 1, pp. 1–8, Oct. 2016.

[263] B. A. Kuzubasoglu, E. Sayar, and S. K. Bahadir, "Inkjet-printed CNT/PEDOT:PSS temperature sensor on a textile substrate for wearable intelligent systems," *IEEE Sens. J.*, pp. 1–1, Mar. 2021.

[264] Y. F. Wang *et al.*, "Fully Printed PEDOT:PSS-based Temperature Sensor with High Humidity Stability for Wireless Healthcare Monitoring," *Sci. Rep.*, vol. 10, no. 1, pp. 1–8, Dec. 2020.

[265] A. Al-Halhouli *et al.*, "Clinical Evaluation of Respiratory Rate Measurements on COPD (Male) Patients Using Wearable Inkjet-Printed Sensor," *Sensors*, vol. 21, no. 2, p. 468, Jan. 2021.

[266] A. Al-Halhouli, L. Al-Ghussain, S. El Bouri, H. Liu, and D. Zheng, "Clinical evaluation of stretchable and wearable inkjet-printed strain gauge sensor for respiratory rate monitoring at different measurements locations," *J. Clin. Monit. Comput.*, pp. 1–10, Feb. 2020.

[267] M. Aliqué, C. D. Simão, G. Murillo, and A. Moya, "Fully-Printed Piezoelectric Devices for Flexible Electronics Applications," *Adv. Mater. Technol.*, vol. 6, no. 3, p. 2001020, Mar. 2021.

[268] J. Luo, L. Zhang, T. Wu, H. Song, and C. Tang, "Flexible piezoelectric pressure sensor with high sensitivity for electronic skin using near-field electrohydrodynamic direct-writing method," *Extrem. Mech. Lett.*, p. 101279, Mar. 2021.

[269] S. Khan, S. Ali, A. Khan, M. Ahmed, B. Wang, and A. Bermak, "Inkjet printing of multi-stripes based deflection monitoring sensor on flexible substrate," *Sensors Actuators, A Phys.*, vol. 323, p. 112638, Jun. 2021.

[270] T. K. Kang, "Inkjet printing of highly sensitive, transparent, flexible linear piezoresistive strain sensors," *Coatings*, vol. 11, no. 1, pp. 1–8, Jan. 2021.

[271] M. Jose, M. Lemmens, S. Bormans, R. Thoelen, and W. Deferme, "Fully printed, stretchable and wearable bioimpedance sensor on textiles for tomography," *Flex. Print. Electron.*, vol. 6, no. 1, p. 015010, Mar. 2021.

[272] J. Kwon, Y. Takeda, R. Shiwaku, S. Tokito, K. Cho, and S. Jung, "Three-dimensional monolithic integration in flexible printed organic transistors," *Nat. Commun.*, vol. 10, no. 1, pp. 1–10, Dec. 2019.

[273] S. Wang *et al.*, "Skin electronics from scalable fabrication of an intrinsically stretchable transistor array," *Nature*, vol. 555, no. 7694, pp. 83–88, Mar. 2018.

[274] Z. Li, S. Chang, S. Khuje, and S. Ren, "Recent Advancement of Emerging Nano Copper-Based Printable Flexible Hybrid Electronics," *ACS Nano*, 2019.

[275] A. Khan, K. Rahman, S. Ali, S. Khan, B. Wang, and A. Bermak, "Fabrication of circuits by multi-nozzle electrohydrodynamic inkjet printing for soft wearable electronics," *J. Mater. Res.*, pp. 1–11, Apr. 2021.

[276] Y. M. Fu *et al.*, "An Inkjet Printing Technique for Scalable Microfabrication of Graphene-Based Sensor Components," *IEEE Access*, vol. 8, pp. 79338–79346, Apr. 2020.

[277] S. Sato, T. Enokido, K. Ashikawa, M. Matsubara, K. Kanie, and N. Ohnishi, "Development of a flexible dielectric-barrier-discharge plasma actuator fabricated by inkjet printing using silver nanoparticles-based ink," *Sensors Actuators A Phys.*, vol. 330, p. 112823, Oct. 2021.

[278] A. Banquart *et al.*, "Piezoelectric P(VDF-TrFE) film inkjet printed on silicon for high-frequency ultrasound applications," *J. Appl. Phys.*, vol. 129, no. 19, p. 195107, May 2021.

[279] Y. Brauniger, S. Lochmann, J. Grothe, M. Hantusch, and S. Kaskel, "Piezoelectric Inkjet Printing of Nanoporous Carbons for Micro-supercapacitor Devices," *ACS Appl. Energy Mater.*, vol. 4, no. 2, pp. 1560–1567, Feb. 2021.

[280] M. J. Griffith *et al.*, "Controlling Nanostructure in Inkjet Printed Organic Transistors for Pressure Sensing Applications," *Nanomaterials*, vol. 11, no. 5, p. 1185, Apr. 2021.

[281] Z. Zhu *et al.*, "Additive manufacturing of thin electrolyte layers via inkjet printing of highly-stable ceramic inks," *J. Adv. Ceram.*, vol. 10, no. 2, pp. 279–290, Apr. 2021.

[282] F. Iervolino, R. Suriano, M. Scolari, I. Gelmi, L. Castoldi, and M. Levi, "Inkjet Printing of a Benzocyclobutene-Based Polymer as a Low-k Material for Electronic Applications," *ACS Omega*, vol. 6, no. 24, pp. 15892–15902, Jun. 2021.

[283] E. Carlos *et al.*, "Design and synthesis of low temperature printed metal oxide memristors," *J. Mater. Chem. C*, vol. 9, no. 11, pp. 3911–3918, Mar. 2021.

[284] D. Mitra, R. Thalheim, and R. Zichner, "Inkjet Printed Heating Elements based on Nanoparticle Silver Ink with Adjustable Temperature Distribution for Flexible Applications," *Phys. Status Solidi*, p. pssa.202100257, Jun. 2021.

[285] J. Koo, J. W. Kim, M. Kim, S. Yoon, and J. H. Shim, "Inkjet Printing of Silica Aerogel for Fabrication of 2-D Patterned Thermal Insulation Layers," *Int. J. Precis. Eng. Manuf. - Green Technol.*, vol. 8, no. 2, pp. 445–451, Mar. 2021.

[286] P. Patil, S. Patil, P. Kate, and A. A. Kulkarni, "Inkjet printing of silver nanowires on flexible surfaces and methodologies to improve the conductivity and stability of the printed patterns," *Nanoscale Adv.*, vol. 3, no. 1, pp. 240–248, Jan. 2021.

[287] L. Ghorbani and M. Rabbani, "Fabrication of a time-temperature indicator by inkjet printing of a spore-based bio-ink," *Bioprinting*, vol. 21, p. e00109, Mar. 2021.

[288] S. Uzun *et al.*, "Additive-Free Aqueous MXene Inks for Thermal Inkjet Printing on Textiles," *Small*, vol. 17, no. 1, p. 2006376, Jan. 2021.

[289] Q. Jing *et al.*, "Aerosol-jet-printed, conformable microfluidic force sensors," *Cell Reports Phys. Sci.*, vol. 2, no. 4, p. 100386, Apr. 2021.

[290] T. T. T. Can, Y. J. Kwack, and W. S. Choi, "Drop-on-demand patterning of MoS2 using electrohydrodynamic jet printing for thin-film transistors," *Mater. Des.*, vol. 199, p. 109408, Feb. 2021.

[291] W. Zou, H. Yu, P. Zhou, Y. Zhong, Y. Wang, and L. Liu, "High-resolution additive direct writing of metal micro/nanostructures by electrohydrodynamic jet printing," *Appl. Surf. Sci.*, vol. 543,

p. 148800, Mar. 2021.

[292] X. Zhang, X. Jiang, Z. Zhang, and H. Qin, "Fabrication of silver microstructures via electrohydrodynamic inkjet printing as customizable X-ray marker in bio-structure for biomedical diagnostic imaging," *Int. J. Adv. Manuf. Technol.*, vol. 114, no. 1–2, pp. 241–250, May 2021.

[293] L. Jiang *et al.*, "Electrohydrodynamic printing of a dielectric elastomer actuator and its application in tunable lenses," *Compos. Part A Appl. Sci. Manuf.*, vol. 147, p. 106461, Aug. 2021.

[294] F. Zheng, B. Derby, and J. Wong, "Fabrication of microvascular constructs using high resolution electrohydrodynamic inkjet printing," *Biofabrication*, vol. 13, no. 3, p. 35006, Jul. 2021.

MUHAMMAD ALI SHAH received B.Sc degree in Electronics Engineering from COMSATS Institute of Information Technology, Pakistan, in 2012. In 2016, he received his M.S. degree in Interdisciplinary Program in Creative Engineering from Korea University of Technology and Education (KOREATECH), Cheonan, Republic of Korea. He worked on MEMS inertial sensors during his Masters studies. After his M.S. degree, Muhammad A. Shah joined Shinsung C&T Co., Ltd, Seoul, Republic of Korea, as an MEMS engineer, where he worked on designing MEMS inertial sensors and microphones. Currently, he is pursuing PhD in Nano-mechatronics at Korea Institute of Machinery and Materials (KIMM) / University of Science and Technology (UST), with piezoelectric inkjet printheads and acoustic printing technology as the core subjects. His research interests include printing technologies, MEMS, wearable, and flexible devices.

DUCK-GYU LEE received his B.S. degree from Dongguk University in 2005 and Ph.D degree from Seoul National University in 2010 all in mechanical engineering. He is now a senior researcher at Korea Institute of Machinery and Materials. His research interests include microfluid mechanics and its application to the industry such as inkjet printing.

BO-YEON LEE is a senior researcher of Department of Nature-Inspired System and Application at Korea Institute Machinery and Materials. She earned her Ph.D. degree in Electrical and Computer Science from Seoul National University, Korea in 2018. She received her B.S. degree in Electrical Engineering from Pusan National University, Korea in 2012. Her recent research interests include skin-inspired tactile sensors and 3D printed flexible electronics.

SHIN HUR received B.Sc degree in Mechanical Engineering from Jeonbuk National University, Jeonju, Republic of Korea, in 1987. In 1989, he received his M.S. degree in Mechanical Engineering from Jeonbuk National University, Jeonju, Republic of Korea. He worked on translational control of one-link elastic arm with a tip mass during his Masters studies. After his M.S. degree, he received his PhD degree in Mechanical Engineering from Chungnam National University, Daejeon, Republic of Korea in 2005. He worked on evaluations and measurements of mechanical properties of nanoscale polymer film during his PhD studies. He joined Korea Institute of Machinery and Materials (KIMM) in Daejeon, Republic of Korea in 1991 as a researcher, and is currently working as a principal researcher. His research interests include inkjet printing technologies, acoustic sensors, MEMS devices and acoustic metamaterial devices.